

**The Innate Reactivity of a Membrane Associated Peptide  
Towards Lipids: Acyl Transfer to Melittin Without Enzyme  
Catalysis**

Journal:	<i>Organic &amp; Biomolecular Chemistry</i>
Manuscript ID:	OB-ART-12-2011-007113.R1
Article Type:	Paper
Date Submitted by the Author:	n/a
Complete List of Authors:	Dods, Robert; Durham University, Chemistry Mosely, Jackie; University of Durham, Department of Chemistry Sanderson, John; University Science Laboratories, Dept of Chemistry
Note: The following files were submitted by the author for peer review, but cannot be converted to PDF. You must view these files (e.g. movies) online.	
Scheme_1_Rxn_Mech_RSC.cdx	

# The Innate Reactivity of a Membrane Associated Peptide Towards Lipids: Acyl Transfer to Melittin Without Enzyme Catalysis

Robert H Dods,<sup>‡a</sup> Jackie A Mosely<sup>\*a</sup> and John M Sanderson<sup>\*a</sup>

Received (in XXX, XXX) Xth XXXXXXXXX 200X, Accepted Xth XXXXXXXXX 200X

First published on the web Xth XXXXXXXXX 200X

DOI: 10.1039/b000000x

The innate reactivity of the peptide melittin (H-GIGAVLKVLTTGLPALISWIKRKRQQ-NH<sub>2</sub>) towards membrane lipids has been explored using LC-MS methods. The high sensitivity afforded by LC-MS analysis enabled acyl transfer to the peptide to be detected, within 4 h, from membranes composed of phosphocholines (PCs). Acyl transfer from PCs was also observed from mixtures of PC with phosphoserine (PS) or phosphoglycerol (PG). In the latter case, transfer from PG was also detected. The half-lives for melittin conversion varied between 24 h and 75 h, being fastest for POPC and slowest for DOPC/DMPG mixtures. The order of reactivity for amino groups on the peptide was N-terminus > K23 >> K21 > K7. Products arising from double-acylation of melittin were detected as minor components, together with a putative component derived from transesterification involving S18 of the peptide.

## Introduction

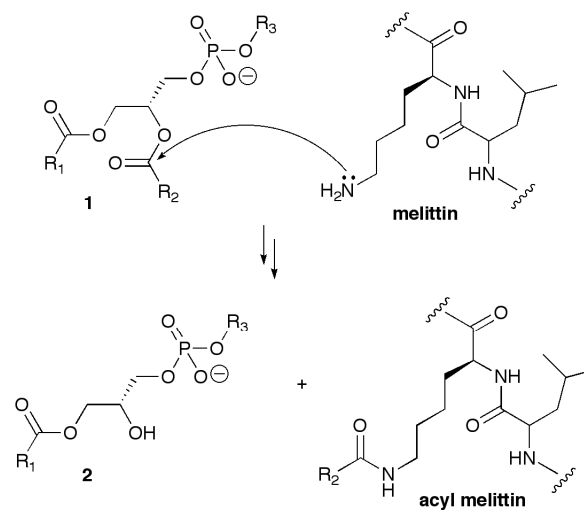
Despite enzyme-catalysed protein lipidation reactions being well established,<sup>1,2</sup> acyl group transfer from lipids to proteins in the absence of enzyme catalysis is poorly characterised. Any notion that the lipid membrane may be considered a chemically inert medium, in respect of the proteins and peptides associated with it, was recently challenged by the observation of innate reactivity between the peptide melittin and membranes composed of phosphocholines.<sup>3</sup> This reactivity was identified through the detection of acylated melittin in MALDI-ToF MS spectra of synthetic (*i.e.* enzyme-free) melittin-lipid mixtures. Whilst the MALDI-ToF MS method was sufficiently sensitive to detect both products of the reaction, namely the acylated melittin itself and the *lysophosphocholine* byproduct **2** (Scheme 1), it was of insufficient sensitivity to detect reaction products in the early stages after addition of melittin to membranes. It was therefore desirable to develop a more sensitive analytical LC-based method to address sensitivity issues and facilitate quantification of the reaction at each of the available sites of the peptide with a range of lipids. The resulting LC-MS method, which is of sufficient sensitivity to detect acylation with 4 h of peptide addition, as well as the presence of previously undetected reaction products, is reported herein.

### 1-Palmitoyl-2-Oleoyl-3-Phosphocholine (POPC)

#### Separation of Acylated Melittin by Liquid Chromatography

All experiments were conducted by incubating melittin and unilamellar liposomes of 100 nm diameter at 37 °C in high salt buffers. Sodium bicarbonate at pH 7.4 was employed as buffer, as this is suitably volatile for MS analyses and permits good chromatographic separation by reverse-phase LC. LC-MS analyses using a C<sub>18</sub> column gave good separation of unreacted melittin, acylated melittin and both *lysophosphocholines* (Fig.

1A). The separated components were detected using a photodiode array (PDA) detector and an ESI FTICR mass spectrometer (further details in the supporting information).



POPC: R<sub>1</sub> = palmitoyl, R<sub>2</sub> = oleoyl, R<sub>3</sub> = CH<sub>2</sub>CH<sub>2</sub>NMe<sub>3</sub>  
 OPPC: R<sub>1</sub> = oleoyl, R<sub>2</sub> = palmitoyl, R<sub>3</sub> = CH<sub>2</sub>CH<sub>2</sub>NMe<sub>3</sub>  
 DOPC: R<sub>1</sub> = R<sub>2</sub> = oleoyl, R<sub>3</sub> = CH<sub>2</sub>CH<sub>2</sub>NMe<sub>3</sub>  
 DMPG: R<sub>1</sub> = R<sub>2</sub> = myristoyl, R<sub>3</sub> = CH<sub>2</sub>CH(OH)CH<sub>2</sub>OH  
 DPPS: R<sub>1</sub> = R<sub>2</sub> = palmitoyl, R<sub>3</sub> = CH<sub>2</sub>CH(NH<sub>2</sub>)CO<sub>2</sub>H

Scheme 1 Generalised reaction between melittin and phospholipids.

It was striking that six acyl melittin peaks could be detected in the LC trace, with two of these predominating (peaks v and vi, Fig. 1A). For most experiments, LC analyses were performed using injection quantities that were insufficient for peak detection by UV methods. However, some analyses (for higher order MS<sup>n</sup> experiments) were conducted with a higher loading that permitted a comparison of the peaks arising from the total absorbance of the PDA detector with those of the ion current (Fig. 1A and B). With the assumption that acylation did not significantly modify the extinction coefficient of the

peptide, this comparison indicated that the ionisation efficiency of the acylated products differed significantly.

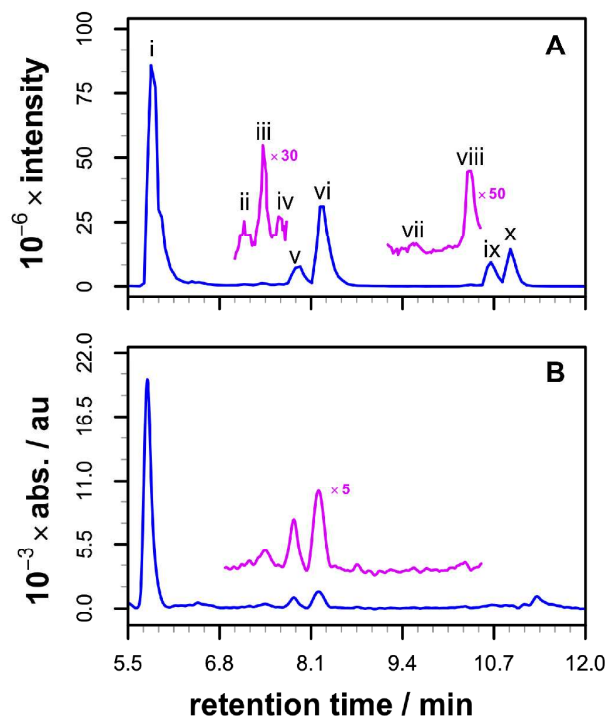


**Fig. 1** LC chromatograms from a mixture of melittin (45  $\mu\text{M}$ ) and POPC (0.25 mM) at 37  $^{\circ}\text{C}$  in 10 mM  $\text{NaHCO}_3$ /90 mM NaCl, after 52 h. Separation was performed using an Xbridge C18 column (Waters), with a linear reverse-phase gradient over 12 min. (A) total ion chromatogram (TIC), plotted as absolute intensity; (B) total PDA absorbance. Peak i is melittin; ii–vii are acylated melittin; viii–x are *lyso*-PC.

This was most notable for peaks iii and vi, both of which had different relative peak areas from the PDA when compared with those determined by ion intensity. It was nevertheless apparent that both the PDA and total ion chromatograms (TICs) gave the same trend in relative peak area for each of the peptides in the mixture, with peak vi being the predominant acylated melittin in both cases. Relative peak areas from the MS chromatogram (Fig. 1A) could therefore be interpreted in a semi-quantitative manner to assess the amount of each of the compounds present.

Analysis of extracted ion chromatograms (EICs) revealed that each of the two possible *lyso*-PCs eluted as two peaks (see ESI). The major peak in each case had a longer retention time and was attributed to the 1-acyl *lyso*-PC. The minor peak was attributed to the 2-acyl *lyso*-PC, with the two *lyso*-PCs existing in equilibrium by transesterification.<sup>4</sup> Peak viii (Fig. 1A) is the minor peak corresponding to 2-palmitoyl-PC. The corresponding minor peak for 2-oleoyl-PC is masked by the major peak for 1-palmitoyl-PC (peak ix).

#### Product Identification by MS and Tandem MS Methods

Acylated melittin products were easily identifiable through the observation of molecular ion charge state series  $[\text{M} + n\text{H}]^{n+}$  where  $n = 3-5$ , corresponding to the addition of either an oleoyl or a palmitoyl group (Fig. 2). In addition to these

multiply charged ions, smaller ions corresponding to in-source fragments were seen in all spectra. The major in-source fragmentation product resulted from  $\gamma$ -type cleavage at P14. Therefore, for melittin and melittin acylated N-terminal to P14, the major fragment had an  $m/z$  of 812, corresponding to the unmodified C-terminal fragment.

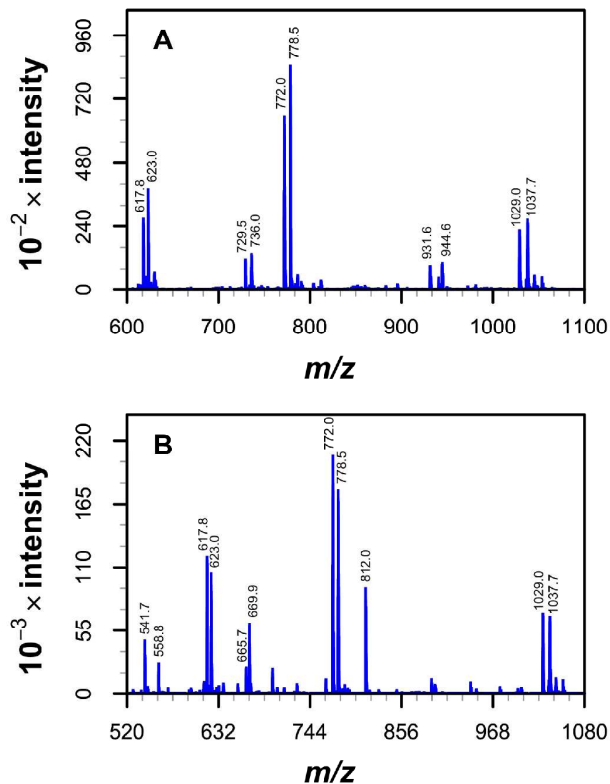


**Fig. 2** MS spectra (absolute intensity) summed over peak v (A) and peak vi (B). Ions are identified as  $[\text{M} + n\text{H}]^{n+}$ , where  $n=3-5$ , for palmitoyl melittin ( $m/z$  1029.0, 772.0, and 617.8) and oleoyl melittin ( $m/z$  1037.7, 778.5, and 623.0). In (A), ions with  $m/z$  944.6 and 736.0 are oleoylated in-source fragments; ions with  $m/z$  931.6 and 729.5 are the corresponding palmitoylated fragments. In (B), ions of  $m/z$  812.0, 669.9, 665.7, 558.8 and 541.7 are unacylated in-source fragments.

For melittin acylated on the C-terminal half of the sequence, this  $\gamma$ -type fragment was observed with  $m/z$  932 (palmitoyl) or 945 (oleoyl). This provided clear indication of the region of the peptide to which acyl transfer had occurred even before any other analyses such as tandem MS had been performed. Tandem MS (MS/MS) was performed on the  $[\text{M} + 4\text{H}]^{4+}$  charge state for acylated melittin ( $m/z$  772 and 778 for palmitoyl and oleoyl respectively). This yielded clear sequence ladders of  $\gamma$ -type and  $\beta$ -type fragments that permitted unambiguous identification of peak vi as the N-terminal acylated peptide (Fig. 3A) and peak v as the peptide modified at K21 or K23 (Fig. 3B). The product ion of  $m/z$  976.6 in the MS/MS spectrum of the palmitoylated precursor in peak vi (Fig. 3A) was further fragmented to yield a very clean sequence ladder of  $\beta$ -type ions matching N-terminal acylation (Fig. 3C), which both confirmed this assignment and ruled out this peak in the LC trace arising by modification at other sites.

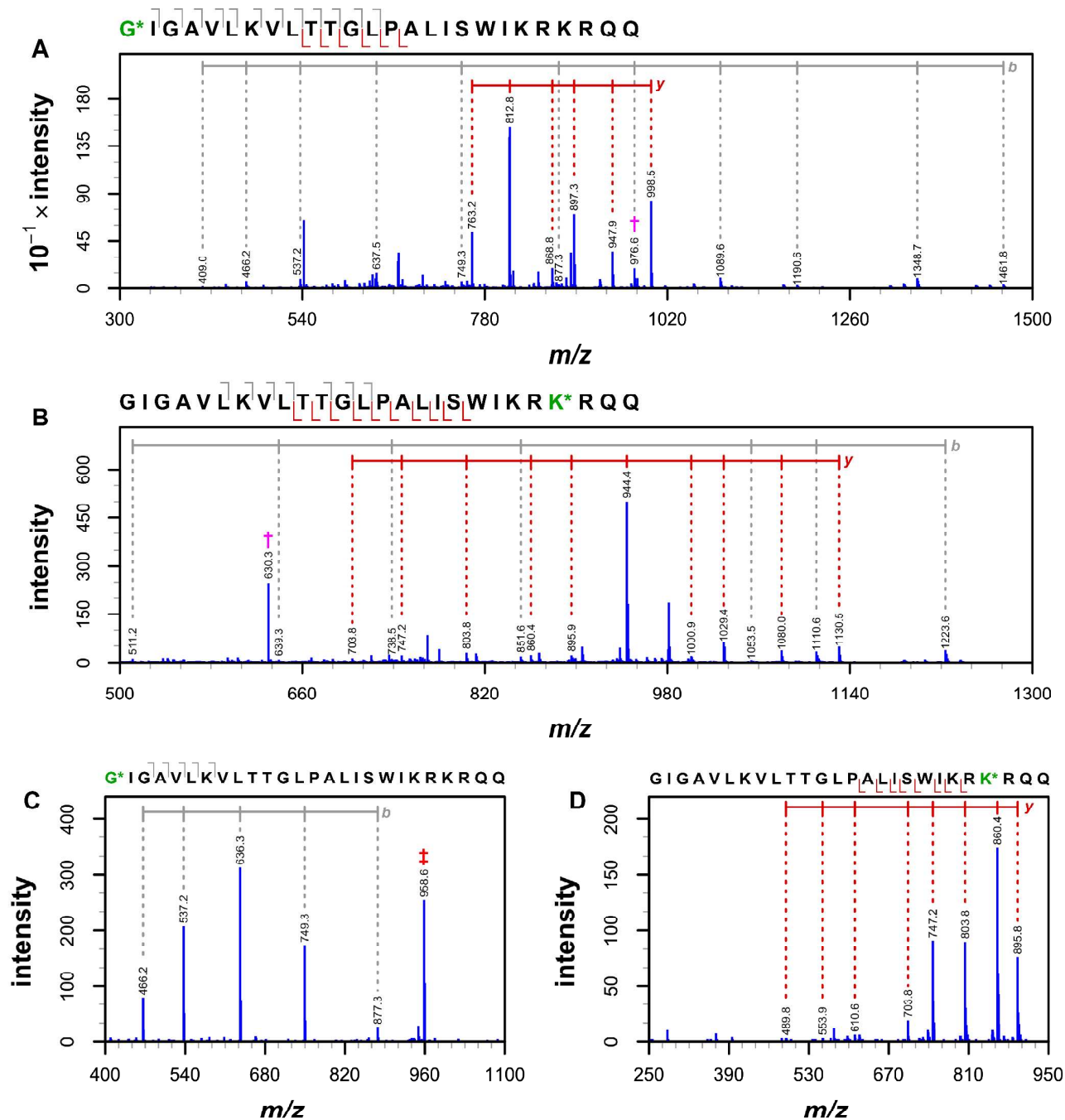


**Fig. 3** Higher level MS analyses of peaks v and vi (Fig. 1): (A) MS/MS of peak vi, precursor ion  $m/z$  772.0; (B) MS/MS of peak v, precursor ion  $m/z$  778.5; (C) MS<sup>3</sup> of peak vi, precursor ion  $m/z$  976.6 (indicated by a dagger in Fig. 3A) from MS/MS of peak vi. The peak indicated with a double dagger corresponds to the parent-H<sub>2</sub>O; (D) MS<sup>3</sup> of peak v, precursor ion  $m/z$  630.3 (indicated by a dagger in Fig. 3B) from MS/MS of peak v. Residues (G\*, K\*) matching the site of modification are indicated by asterisks. Data are presented as absolute intensity. Full assignments are given in the ESI.

The product ion of  $m/z$  630.3 in the MS/MS spectrum of the oleoylated component in peak v was also fragmented, yielding a sequence ladder of y-type fragments that extended sufficiently close to the C-terminus to rule out modification of K21. Peak v was therefore assigned as the product arising from acylation of K23.

#### Progress of the reaction with POPC

Analysis by LC-MS offered the possibility of monitoring the

processes of palmitoylation and oleoylation separately, enabling a comparison of the reactivity of the fatty acyl groups at each position of the lipid. In practice, only the three major peaks in the LC trace corresponding to melittin (peak i), N-acyl melittin (peak vi) and K23-acyl melittin (peak v) were monitored in these experiments, which were conducted using smaller quantities of material per injection than those used for the chromatogram in Fig. 1. Nevertheless, it was striking that the presence of N-acyl melittin could be detected within 4 h

(Fig. 4A).

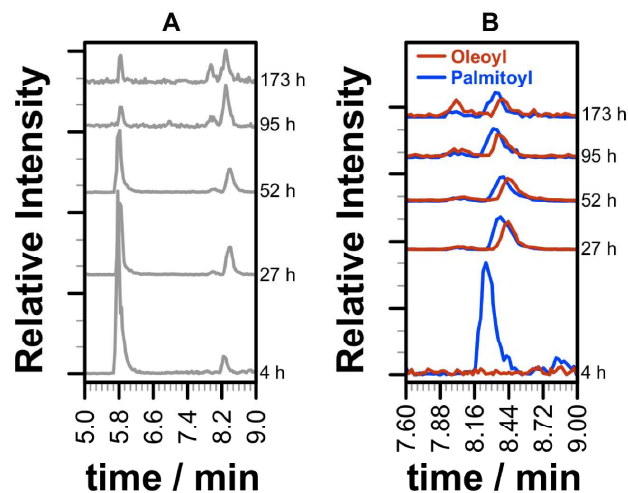


**Fig. 4** Change in LC profile over time for the reaction of melittin with POPC (conditions as Fig. 1). In each case, the total integrated peak area has been normalised between runs for those peaks visible in the plot. (A) combined extracted ion chromatograms (EICs) for melittin and acylated melittin. (B) EICs for oleoyl and palmitoyl melittin.

Examination of the EICs (Fig. 4B) revealed that the first detectable product, after 4 h, was N-palmitoyl melittin. This can be accounted for by either the N-palmitoyl species forming first, or a propensity for the palmitoylated peptide to ionise more easily by electrospray than its oleoyl counterpart, the effects of which will be more pronounced at low concentrations. As a consequence, no firm conclusions can be made regarding the selectivity of product formation in the early stages. In the later stages of the reaction, it is clear that a significant degree of conversion is achieved, and that the reaction displays subtle lipid regioselectivity. This is most evident when comparing the palmitoyl and oleoyl traces after 95 h and 173 h (Fig. 4B), where the fatty acyl selectivities for reaction at the N-terminal amino and K23 amino groups are opposed, with oleoylation of K23 preferred and palmitoylation of the N-terminal amino group marginally favoured.

#### Minor products in the reaction with POPC

Three minor monoacylated products could be detected, (peaks ii-iv, Fig. 1), albeit with very weak intensities. The presence of these components was more evident upon examination of the LC-MS<sup>3</sup> traces for these samples (Fig. 5). Although the ion currents were understandably low, the higher order MS<sup>n</sup> experiments yielded significant improvements in the signal-to-noise ratio in these analyses. Where the ion corresponding to  $m/z$  972 was used as the precursor ion for MS<sup>3</sup> experiments (Fig. 5A), all three of the minor peaks (ii-iv) were resolved. When the MS<sup>3</sup> precursor ion at  $m/z$  630.2 was used however (Fig. 5B), peak iv was absent. This implies that the MS/MS precursor ion ( $m/z$  772) for peak iv did not fragment to yield a product ion with  $m/z$  630.2, suggesting that peak iv corresponds to a product acylated N-terminal to P14. On the other hand, peaks ii and iii both yielded a product ion with  $m/z$  630.2, suggesting that they are both products modified in the C-terminal portion of the peptide after P14.

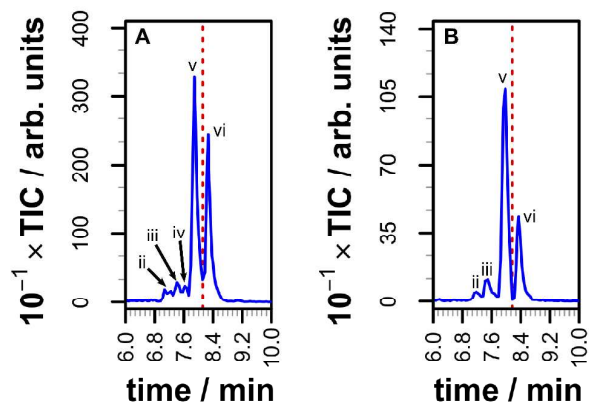


**Fig. 5** TICs for MS level 3 in analyses of POPC/melittin. Peak labels correspond to those of Fig. 1. (A) MS/MS precursor  $m/z$  772; MS<sup>3</sup> precursor to the left of the dotted line  $m/z$  972 and  $m/z$  976 to the right. (B) MS/MS precursor  $m/z$  778; MS<sup>3</sup> precursor to the left of the dotted line  $m/z$  630.2 and  $m/z$  1115.5 to the right.

The observation of all of peaks ii-iv in Fig. 5A can be attributed to the precursor ion of  $m/z$  972 being a y-type fragment of sufficient size to cover all of the internal lysines and the C-terminus of the peptide. On the basis of mass spectra from these peaks (see ESI), peak iv has been tentatively assigned as the product of acylation at K7 and peak iii as acylation at K21. The remaining peak was difficult to assign, although the product ion sequence ladder indicated that it was modified at, or C-terminal to, S18. On the basis of the available sites of reaction, we propose that this product arises by acylation of S18 in a transesterification reaction. In previous work using MALDI-ToF MS, doubly acylated peptides were not detectable in the mixture.<sup>3</sup>

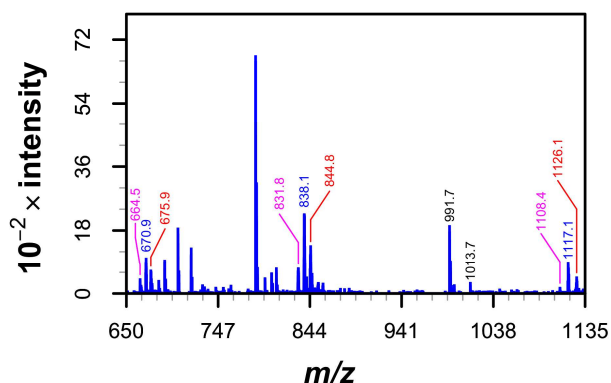


**Fig. 6** Mass spectrum (absolute intensity) averaged over RT 10:00-10:40 (peak vii, Fig. 1), showing the presence of ions corresponding to doubly acylated melittin, [(Melittin + 2Acyl - 2H) +  $nH$ ]<sup>n+</sup>, where  $n=3-5$ .

However, the improvements in sensitivity offered by LC separation combined with electrospray MS enabled these products to be identified over a wide span of retention time (9.5–11.5 min, Fig. 6) that included peak vii. For each charge state, a group of three ions was observed, corresponding to doubly oleoylated, singly oleoylated plus singly palmitoylated, and doubly palmitoylated melittin, in descending order of  $m/z$ . In principle, assuming reaction of 2

acyl groups at 4 potential sites, a total of 24 distinct doubly acylated peptides could result. Given the effects of single substitutions at different positions on retention time (Fig. 5), the corresponding extracted ion chromatograms for doubly-acylated melittin were understandably complex (see ESI). Added to this, the retention times for some of the doubly acylated peptides overlapped those of the *lyso*-PCs, with potential effects on the magnitude of the ion currents observed. This made precise quantification of the extent of double acylation difficult. Our best estimate for the proportion of doubly acylated product, based on the PDA (Fig. 1) and extracted ion chromatogram data, is  $\leq 10\%$ .

## Acyl Transfer From Other Lipids

### 1-Oleoyl-2-Palmitoyl-3-Phosphocholine (OPPC)

The reaction between melittin and membranes composed of OPPC was followed to determine whether the small degree of selectivity found with POPC was attributable to the position on the glycerol backbone, or the chemical nature of the acyl group. The data (Fig. 7) indicated that the overall rate of reaction was marginally slower to that observed for POPC.

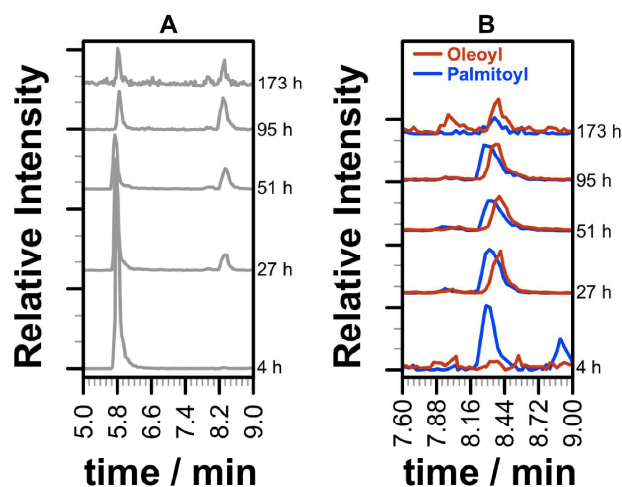


**Fig. 7** LC profiles for the reaction with OPPC (conditions as Fig. 1). The total integrated peak area is normalised between runs for those peaks visible in the plot. (A) TICs for melittin and acylated melittin. (B) EICs for oleoyl and palmitoyl melittin.

Oleoylation of K23 was still marginally favoured over palmitoylation, suggesting that the identity of the acyl group had some influence on the reactivity at this position. As with POPC, selectivity for reaction at the N-terminal amino group of melittin was minimal, with a marginal preference for transfer of the acyl group at the 1-position of glycerol.

### 1,2-dioleoyl-3-phosphocholine (DOPC)/1,2-dipalmitoyl-3-phosphoserine (DPPS), 4:1

This lipid mixture was examined in order to determine whether the reaction could be extended to classes of lipid other than PCs. In particular, negatively charged lipids have been shown to enhance the membrane binding of melittin, with the bound peptide exhibiting restricted conformational freedom when compared with PC membranes. Interestingly,

with this lipid mixture, acyl transfer was only observed from the PC component (Fig 8).

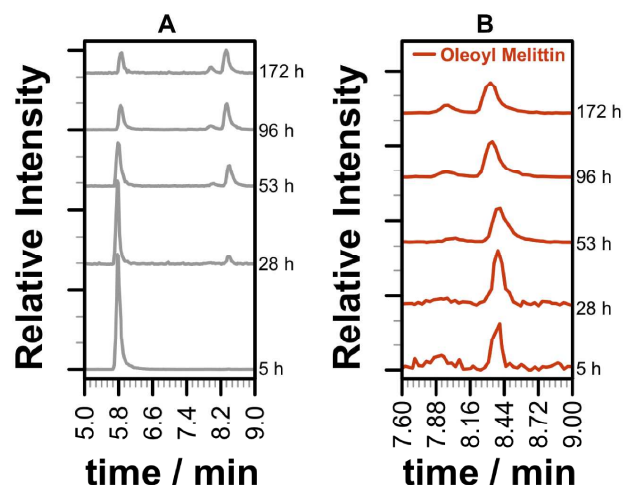


**Fig. 8** LC profile for the reaction with DOPC/DPPS (conditions as Fig. 1). In each case, the total integrated peak area is normalised between runs for those peaks visible in the plot. (A) TICs for melittin and acylated melittin. (B) EICs for oleoyl melittin (palmitoyl melittin was not detected).

This selectivity for PC over PS indicates that mode of binding and orientation of the peptide with regard to individual lipid components is fundamental in determining its surface reactivity.

### DOPC/1,2-dimyristoyl-3-phosphoglycerol (DMPG), 4:1

The effects of lipid composition on the reaction were extended to mixtures of PC with PG (Fig. 9).

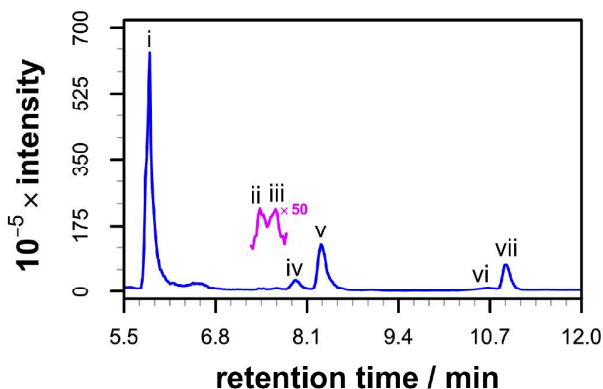


**Fig. 9** LC chromatogram (TIC) for the reaction of melittin (45  $\mu\text{M}$ ) with DOPC/DMPG (4:1, 0.25 mM) after 52 h at 37  $^{\circ}\text{C}$  in 10 mM  $\text{NaHCO}_3$ /90 mM NaCl. Analysis was performed using the same conditions as Fig. 1. Peak i is melittin; peaks ii to v are acylated melittin; peaks vi and vii are *lyso*-PC/*lyso*-PG.

Upon examination of the melittin/DOPC/DMPG mixture, it was evident that products of acyl transfer from both DOPC and DMPG could be detected (Fig 9). In this case, the difference in retention times between equivalent oleoylated and myristoylated peptides was such that the N-terminal myristoylated peptide co-eluted with the K23 oleoylated peptide (Fig. 9, peak iv). Using extracted ion data it was

possible to detect myristoyl transfer from PG within 95 h, and oleoyl transfer from PC within 28 h, a somewhat slower rate than found with any of the other lipid mixtures.

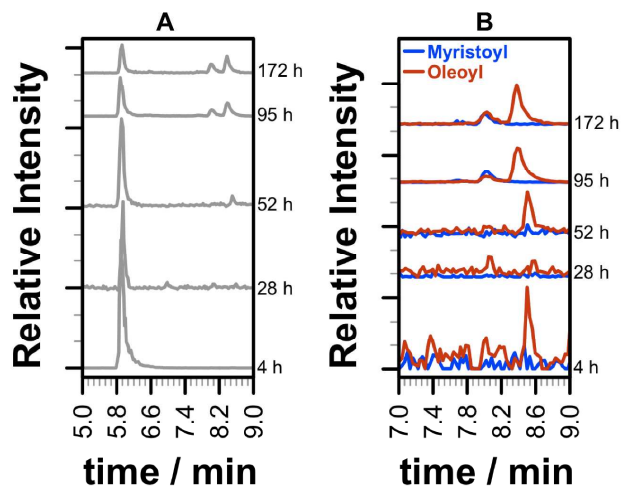


**Fig. 10** LC profiles for the reaction with DOPC/DMPG (4:1, conditions as Fig. 1). The total integrated peak area is normalised between runs for those peaks visible in the plot. (A) TICs for melittin and acylated melittin. (B) EICs for oleoyl and myristoyl melittin.

This slower rate may be attributable to a change in binding exhibited by melittin in the presence of PG, but it is nevertheless interesting to note from a fundamental point of view that the reaction is not restricted to PC lipids.

### Comparison of Reaction Rates

As discussed above, the LC peak areas from ion chromatograms give only a semi-quantitative report of the amounts of product present, and consequently the reaction rate. Nonetheless, comparison of the peak areas (Fig. 11) from the different reactions described above reveals two general points. Firstly, the reaction with DOPC/DMPG is confirmed as being slower than the others. Secondly, for all of the reactions, apart from that with DOPC/DMPG, the time required for 50% conversion is  $\sim 24$  h, which is significantly faster than that observed previously with POPC in phosphate buffered saline (16 days).<sup>3</sup>

### Discussion

The reactivity of peptidic functional groups (amines, thiols, alcohols) will be determined by their local environment. In order for acyl transfer to occur, reactive groups of the acyl acceptor (peptide) must approach sufficiently close to the carbonyl groups of the lipid acyl chains in a suitably reactive form, *i.e.* as the free amine. Therefore, when considering the relative rates of acyl transfer at different sites on the peptide, the effects of amine basicity on both the intrinsic rate of reaction and partitioning into the membrane have to be considered.

Aminolysis of alkyl esters in water is generally considered to proceed by rapid reversible attack of the amine on the carbonyl centre to form an initial charge-separated tetrahedral intermediate ( $T^\pm$ ) that then converts into a negatively charged

form ( $T^-$ ), either by proton abstraction in reactions proceeding with general base catalysis, or by proton exchange involving water in uncatalysed reactions. Conversion of  $T^\pm$  to  $T^-$  (base catalysed) and the formation or collapse of  $T^-$  (uncatalysed or water catalysed) are expected to be rate determining.<sup>6</sup> Higher rates are favoured by amines with conjugate acids of high pKa (*i.e.* more basic amines).<sup>7</sup>

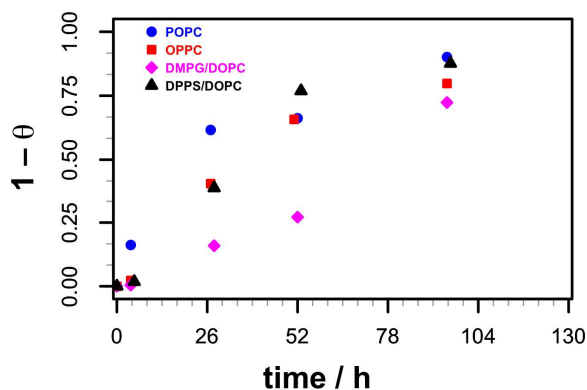


**Fig. 11** Comparison of the rates of acyl transfer with different lipid mixtures. The degree of conversion is expressed as  $1-\theta$ , where  $\theta$  is the melittin peak area divided by the total peak area of melittin + acyl melittin peaks in the ion chromatogram. Errors in  $(1-\theta)$  are  $\pm 0.1$ .

The proportion of the amine that will exist in the neutral form at pH 7.4 will show an inverse relationship with the pKa of the conjugate acid, leading to less penetration of the membrane and reduced reaction rates for more basic amines. The effects of pKa on the rate of acyl transfer are therefore modulated by factors of intrinsic reaction kinetics and membrane penetration that are opposed in their effects.

This raises the question of how the effective pKa values of the ammonium species in the membrane bound state of melittin are able to influence the reaction. Analysis of amino group protonation in melittin is complicated by the existence of monomeric and tetrameric forms of the peptide in equilibrium, with formation of the tetramer promoted at high pH when amino groups are in the neutral state.<sup>8</sup> There is general consensus however, that the N-terminal ammonium group has a pKa in the range 7.5-8.15 in both monomeric and tetrameric states of the peptide in solution.<sup>9,10</sup> One study has addressed the pKa values of the ammonium groups in a micelle-bound state (using monomyristoyl PC) by <sup>15</sup>N NMR, finding a pKa value for the N-terminal ammonium group of 7.9,<sup>10</sup> which is supported by other NMR studies with micelle-associated melittin.<sup>11</sup> This relatively low pKa value for the N-terminal ammonium group indicates that a substantial fraction will be in the neutral form at pH 7.4 and suggests that membrane partitioning is the more important factor for determining the higher reactivity associated with this group. The lysine ammonium groups of K7 and K21 are consistently found with higher pKa values, in the range 9.2-10.2, both for the tetramer in solution and the micelle-associated form.<sup>9,10,8</sup> This is consistent with their low reactivity, compared to the N-terminal amino group, again due to partitioning effects. The greatest discrepancy in measured pKa values occurs for K23, with values ranging from 8.5 to 10.1 for the melittin tetramer

in solution,<sup>8,10</sup> and 10.1 determined for the micelle-associated peptide.<sup>10</sup> Although a pKa of 8.5 is more in keeping with the reactivity of the side chain of K23, the higher value was obtained by more robust NMR methods. An additional factor that will influence reactivity is the membrane disposition of the peptide, which itself will depend on properties such as peptide amphipathicity and membrane composition. In general, in PC membranes the melittin monomer orients with the helices in the plane of the membrane, penetrating to approximately the depth of the glycerol group of the lipid.<sup>12</sup> At higher peptide concentrations, other helix orientations are sampled, including some that appear to be transmembrane, although a substantial fraction of the peptide remains bound in the plane of the membrane.<sup>13</sup> Interestingly, K23 appears to be located in a region with less conformational order,<sup>14</sup> which may account for the greater reactivity seen at this position, as may catalysis from neighbouring basic residues in the sequence. Further complications arise when considering whether bicarbonate ions exert any effect on the rate of reaction. Bicarbonate, along with other bifunctional anions such as the phosphate dianion, is able to function as a catalyst in aminolysis reactions by simultaneously facilitating proton donation to, and abstraction from, the dipolar tetrahedral intermediate ( $T^\ddagger$ ).<sup>15</sup> The increased rates of reaction observed in the presence of bicarbonate suggest that either the anion is able to penetrate sufficiently into the membrane to influence the rate determining step, or that  $T^\ddagger$  is sufficiently solvent exposed to be accessible to the anion.

In the presence of PG or PS, the peptide exhibits a greater affinity for the membrane, and the membrane-associated state samples less conformational space than in PC-only membranes.<sup>13,16</sup> However, studies to address whether melittin association with membranes containing PS or PG leads to demixing (phase separation) of the negatively charged lipid component have produced mixed results, depending to some degree on the nature of the acyl chains of the PC and PG or PS components. Outcomes have ranged from no evidence for demixing of PS in DMPC/DMPS following melittin binding,<sup>17</sup> to demixing of PG in DSPC/DPPG.<sup>18</sup> Our data match a pattern in which binding of melittin to DOPC/DPPS leads to demixing of the PS component, with no subsequent reaction with PS, presumably due to a more peripheral binding of the peptide. On the other hand, melittin binding to DOPC/DMPG behaves in a manner consistent with lipid mixing, with the rate of reaction slowed by the reduced conformational freedom of the peptide and a disposition that is more distal from the lipid acyl carbonyl groups.

## Conclusions

The data presented in this paper, alongside our previous communication, prove unambiguously that peptides are subject to acyl transfer from lipids in the absence of enzyme catalysis. This transfer exhibits some lipid selectivity, and a modest regioselectivity in terms of the available reactive groups on the peptide. Whilst the reaction itself (amine + ester to give amide + alcohol) is not without precedent, the significance in this case is due to the potential impact these findings have on current thinking about the membrane.

Biological membranes cannot be considered as chemically inert; any molecule placed in, or on the surface of, a biological membrane is potentially subject to acyl transfer from one or more of the constituent lipids. This reactivity has been demonstrated using melittin; it is unclear at this stage where melittin lies on the reactivity scale, *i.e.* whether this peptide is typical or atypical of membrane peptides in general. It is to be expected that some sequence motifs and patterns of amphipathicity will favour the reaction by placing the reactive groups in close proximity, in the vicinity of side chains that can provide acid or base catalysis of the reaction. Understanding these parameters will enable a greater depth of understanding of this process.

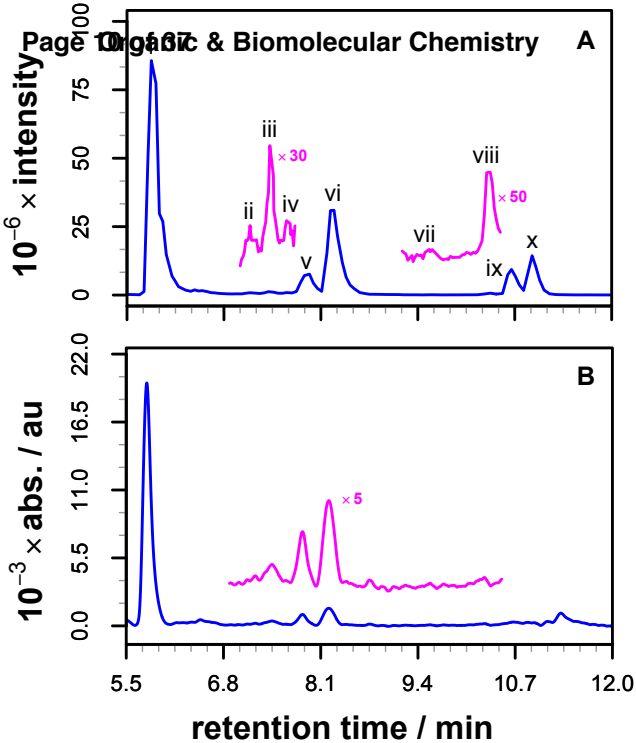
## Notes and references

<sup>a</sup> Department of Chemistry, Biophysical Sciences Institute, Durham University, Durham, United Kingdom. Fax: +44 (0)1913844737; Tel: +44 (0)191 3730838; E-mail: j.m.sanderson@durham.ac.uk

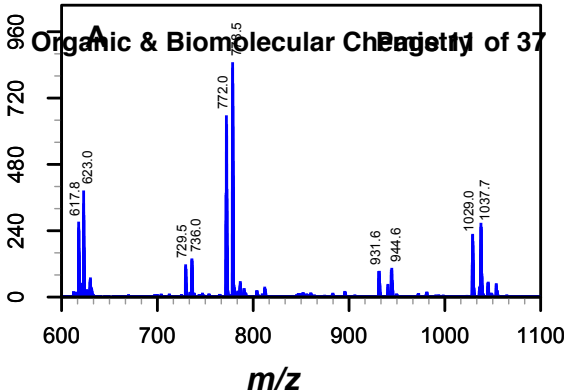
<sup>†</sup> Electronic Supplementary Information (ESI) available: control experiments, full MS data. See DOI: 10.1039/b000000x/

<sup>‡</sup> The authors thank the Biophysical Sciences Institute, Durham University, for a bursary to RHD.

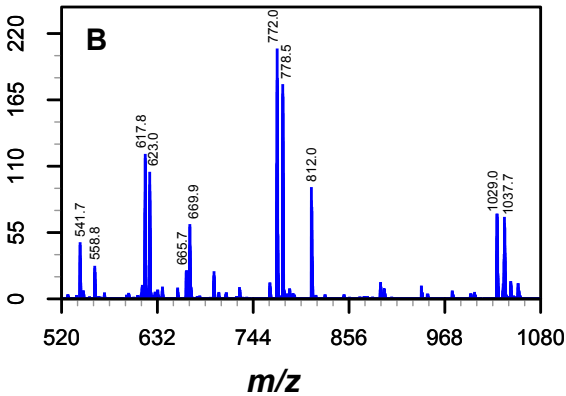
- 1 R. N. Hannoush and J. Sun, *Nat. Chem. Biol.*, 2010, **6**, 498–506; D. O. Martin, E. Beauchamp, and L. G. Berthiaume, *Biochimie*, 2011, **93**, 18–31; L. Li, L. Dong, L. Xia, T. Li, and H. Zhong, *J. Chromatogr. B*, 2011, **879**, 1316–1324.
- 2 W. P. Heal and E. W. Tate, *Org. Biomol. Chem.*, 2010, **8**, 731–738.
- 3 C. J. Pridmore, J. A. Mosely, A. Rodger, and J. M. Sanderson, *Chem. Commun.*, 2011, **47**, 1422–1424.2
- 4 D. Adlercreutz and E. Wehtje, *J. Am. Oil Chem. Soc.*, 2001, **78**, 1007–1011.
- 5 T. J. McIntosh, *Chem. Phys. Lipids*, 2004, **130**, 83–98; C. E. Dempsey and G. S. Butler, *Biochemistry*, 1992, **31**, 11973–11977; M. Monette and M. Lafleur, *Biophys. J.*, 1995, **68**, 187–195; S. Ohki, E. Marcus, D. K. Sukumaran, and K. Arnold, *Biochim. Biophys. Acta*, 1994, **1194**, 223–232;
- 6 A. C. Satterthwait and W. P. Jencks, *J. Am. Chem. Soc.*, 1974, **96**, 7018–7031; M. J. Gresser and W. P. Jencks, *J. Am. Chem. Soc.*, 1977, **99**, 6970–6980.
- 7 I.-H. Um, K.-H. Kim, H.-R. Park, M. Fujio, and Y. Tsuno, *J. Org. Chem.*, 2004, **69**, 3937–3942.
- 8 W. Wilcox and D. Eisenberg, *Protein Sci.*, 1992, **1**, 641–653.
- 9 J. Lauterwein, L. R. Brown, and K. Wuthrich, *Biochim. Biophys. Acta*, 1980, **622**, 219–230; L. Zhu, M. D. Kemple, P. Yuan, and F. G. Prendergast, *Biochemistry*, 1995, **34**, 13196–13202;
- 10 L. Zhu, M. D. Kemple, P. Yuan, and F. G. Prendergast, *Biochemistry*, 1995, **34**, 13196–13202;
- 11 P. Yuan, P. J. Fisher, F. G. Prendergast, and M. D. Kemple, *Biophys. J.*, 1996, **70**, 2223–2238.
- 12 K. Hristova, C. E. Dempsey, and S. H. White, *Biophys. J.*, 2001, **80**, 801–811.
- 13 F. R. Svensson, P. Lincoln, B. Nordén, and E. K. Esbjörner, *Biochim. Biophys. Acta*, 2011, **1808**, 219–228; A. S. Ladokhin and S. H. White, *Biochim. Biophys. Acta*, 2001, **1514**, 253–260.
- 14 Y. H. Lam, S. R. Wassall, C. J. Morton, R. Smith, and F. Separovic, *Biophys. J.*, 2001, **81**, 2752–2761.
- 15 C. C. Yang and W. P. Jencks, *J. Am. Chem. Soc.*, 1988, **110**, 2972–2973.
- 16 M. Monette and M. Lafleur, *Biophys. J.*, 1995, **68**, 187–195.
- 17 C. Dempsey, M. Bitbol, and A. Watts, *Biochemistry*, 1989, **28**, 6590–6596.
- 18 M. Lafleur, J. F. Faucon, J. Dufourcq, and M. Pézolet, *Biochim. Biophys. Acta*, 1989, **980**, 85–92.

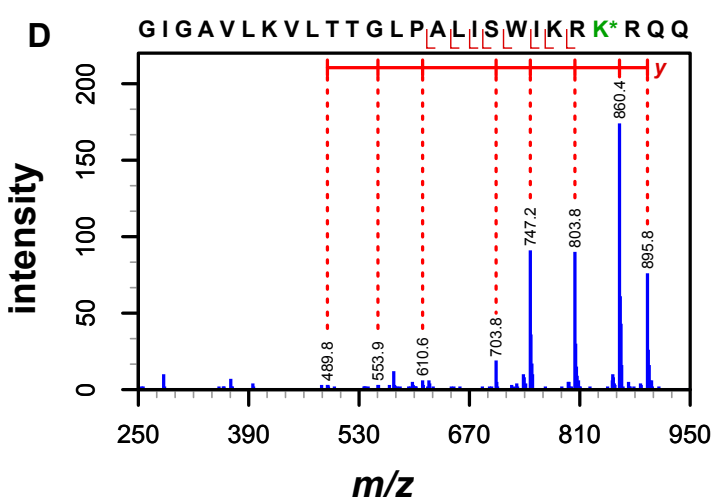
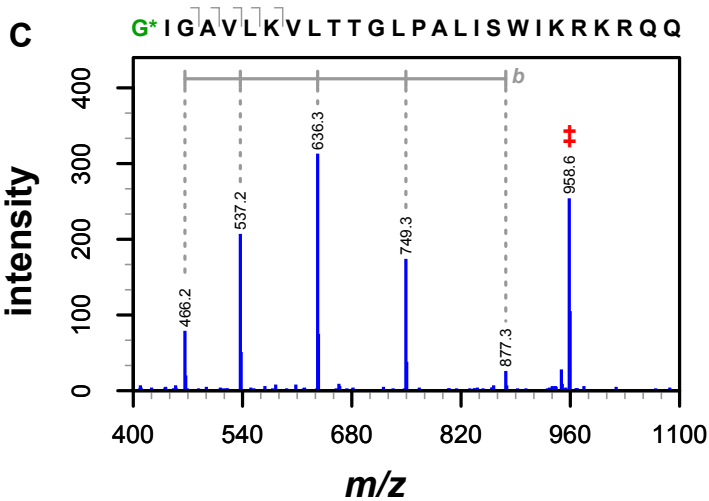
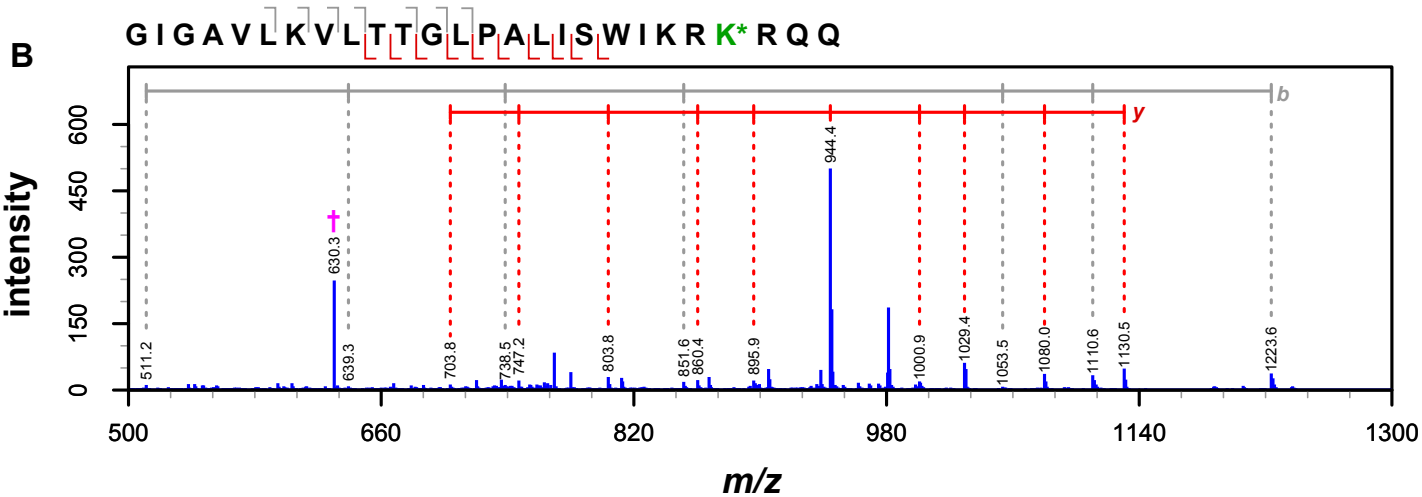
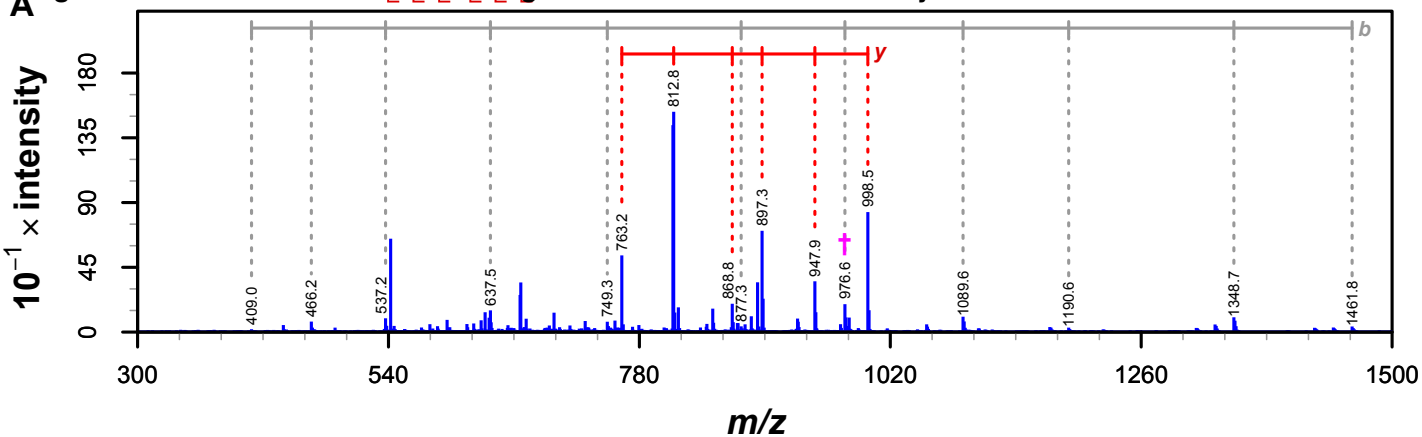


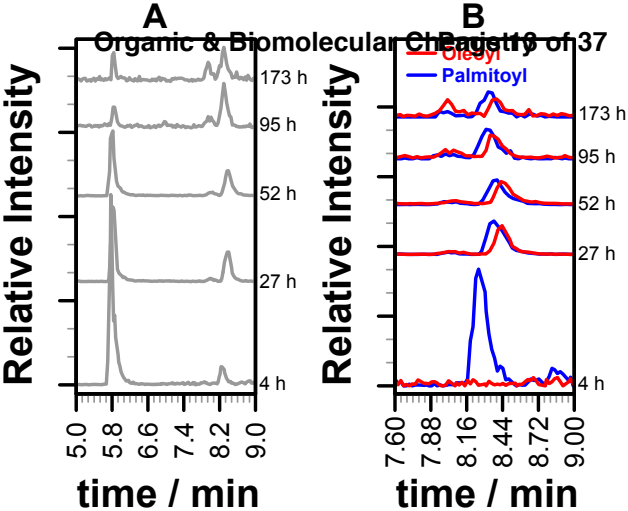
$10^{-2} \times \text{intensity}$

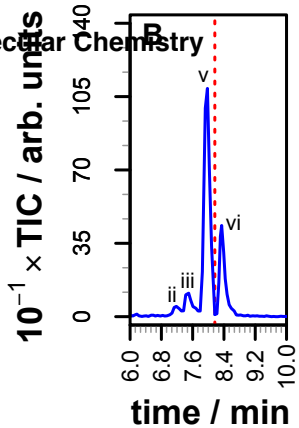
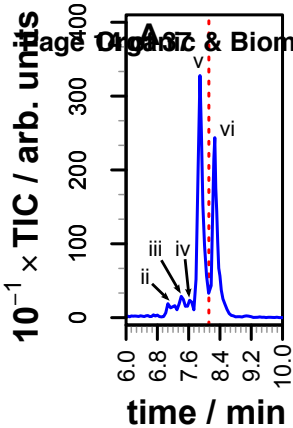


$10^{-3} \times \text{intensity}$

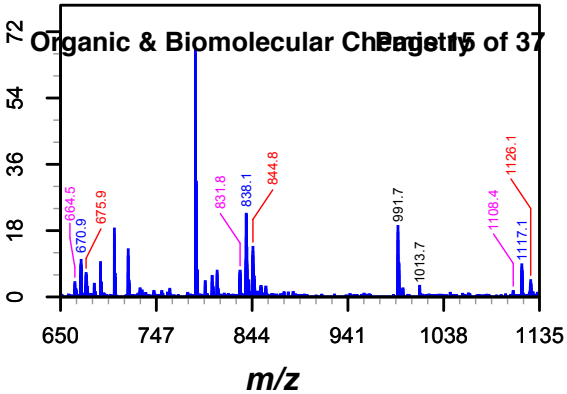




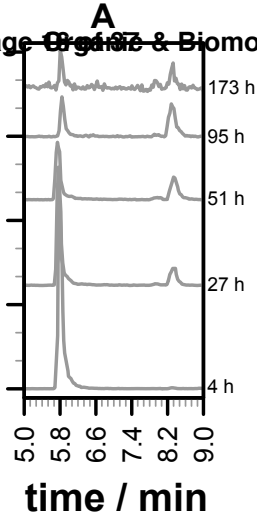




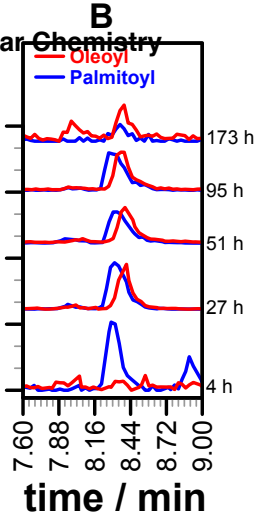
$10^{-2} \times \text{intensity}$



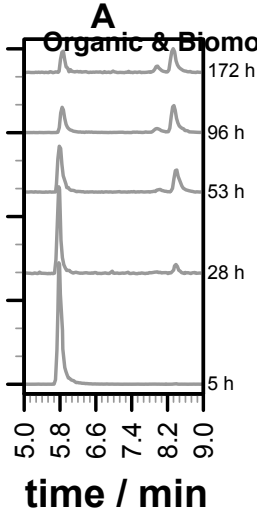
Relative Intensity



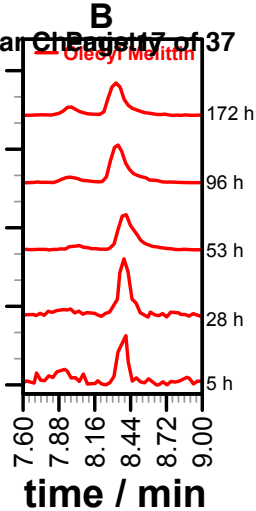
Relative Intensity

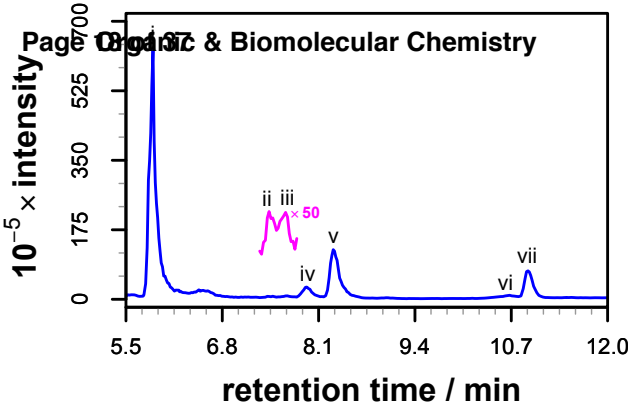


**Relative Intensity**

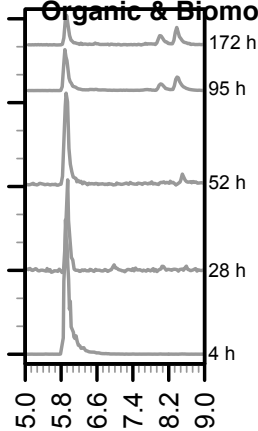


**Relative Intensity**





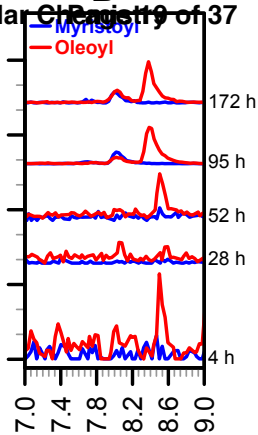
**Relative Intensity**



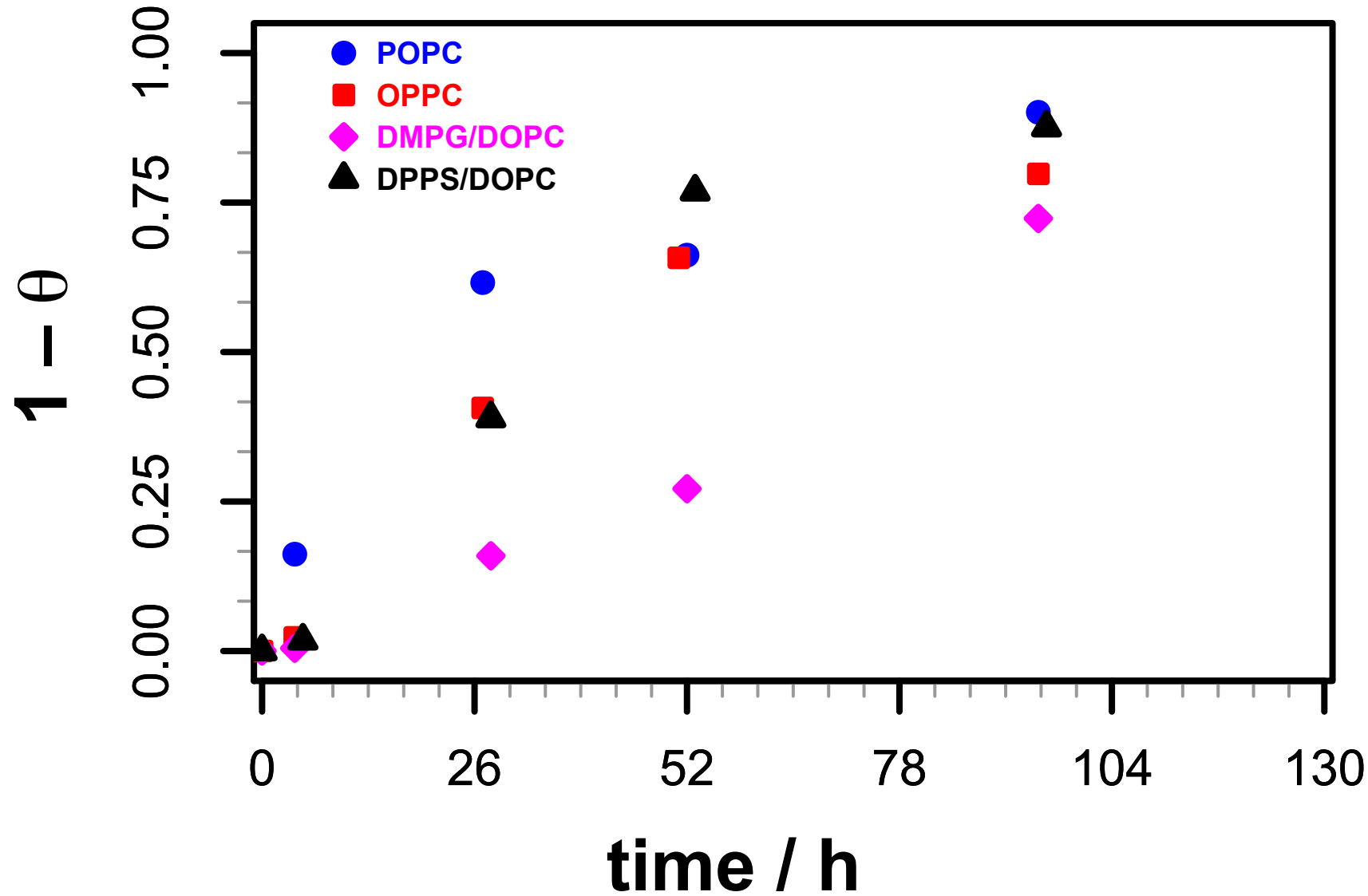
**time / min**

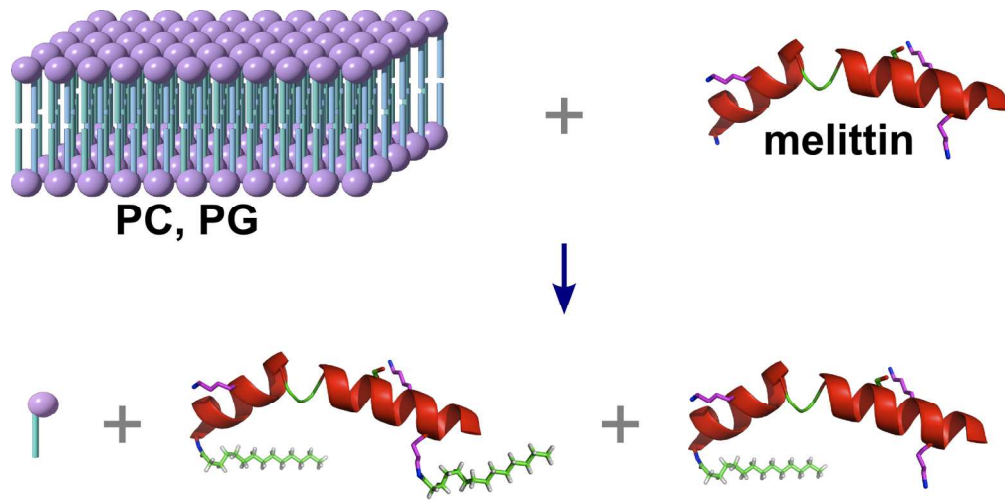
**B**

**Relative Intensity**



**time / min**





# The Innate Reactivity of a Membrane Associated Peptide Towards Lipids: Acyl Transfer to Melittin Without Enzyme Catalysis: Supporting Information

Robert H Dods,<sup>‡a</sup> Jackie A Mosely<sup>\*a</sup> and John M Sanderson<sup>\*a</sup>

## Experimental Methods

### Materials and sample preparation

Synthetic melittin (99.2% by HPLC, Batch No. L15686/b, Alexis brand) was obtained from Enzo Life Sciences (Exeter, UK). Lipids were obtained as dry powders from Avanti Polar Lipids *via* Instruchemie B.V., The Netherlands.

The concentration of melittin in stock solutions was determined by absorption measurements at 280 nm, with the extinction coefficient calculated as  $5570 \text{ M}^{-1} \text{ cm}^{-1}$ .

All experiments were conducted in aqueous buffers at pH 7.4 containing sodium bicarbonate (10 mM) and sodium chloride (90 mM).

Liposomes were prepared by drying a solution of the lipid (typically 165  $\mu\text{l}$  of a 2 mg/ml solution in  $\text{CHCl}_3$ ) *in vacuo* to form a thin film around the side of a round bottomed flask. This film was then hydrated with 1 ml of buffer and after thorough mixing was subjected to five freeze thaw cycles. The vesicles were then extruded 10 times through laser-etched polycarbonate membranes (Whatman, 100 nm pore size) at 60  $^\circ\text{C}$  using a thermobarrel extruder (Northern Lipids, Burnaby, Canada) under a positive  $\text{N}_2$  pressure.

### Melittin acylation

Mixtures (52  $\mu\text{l}$ ) of melittin (46  $\mu\text{M}$ ) and liposomes (0.23 mM) were prepared by adding a solution of the peptide to each liposome dispersion in buffer. Following mixing, mixtures were incubated at 37  $^\circ\text{C}$  throughout each experiment. The pH values of the solutions (pH 7.4) were unchanged after mixing the peptide and liposomes. Control experiments were conducted using melittin without liposomes, and liposomes without melittin. For analysis by LC-MS, 5  $\mu\text{L}$  of the reaction mixture was removed and diluted into 45  $\mu\text{L}$  aqueous medium (20 mM ammonium bicarbonate at pH 7.4).

### Tryptic digests

Calcium chloride (*aq.*, 100 mM, 2.2  $\mu\text{l}$ ) was added to the melittin/liposome mixtures (20  $\mu\text{l}$ ). Trypsin solution (250 ng/ $\mu\text{l}$ , 0.025% acetic acid/50 mM Tris; 1  $\mu\text{l}$ ) was added. The mixture was agitated at 37  $^\circ\text{C}$ . After 18 h, samples were analysed by LC-MS.

### LC-MS

LC MS was performed with a Surveyor HPLC coupled to an LTQFT MS (ThermoFinnigan Corp, Bremen, Germany). Chromatographic separation was achieved from 5  $\mu\text{L}$  sample solution aliquots injected onto an Xbridge 3.5  $\mu\text{m}$  C18, 100 x 2.1 mm column (Waters, Manchester, UK). The 12 minute reverse phase gradient conditions started at 95% ( $\text{H}_2\text{O}$  + 0.1 % formic acid) / 5 % ( $\text{CH}_3\text{CN}$  + 0.1 % formic acid) and finished

at 5 % ( $\text{H}_2\text{O}$  + 0.1 % formic acid) / 95 % ( $\text{CH}_3\text{CN}$  + 0.1 % formic acid) with a mobile phase flow rate of 200  $\mu\text{L min}^{-1}$ . Retention times were reproducible to within  $\pm 0.1$  min. Photodiode array data were recorded over the wavelength range 200–600 nm. The positive ion electrospray signal was optimized: the nitrogen sheath gas was kept between 8–10 arbitrary units, the auxiliary gas and sweep gas were set between 2–4 arbitrary units, as per the manufacturer's software, the capillary was heated to 250  $^\circ\text{C}$  and the spray voltage was held at 4.0 kV. The tube lens voltage was varied to deliver the optimal ion intensity. All full scan MS data were measured in the Fourier-transform ion cyclotron resonance mass analyser surrounded by a 7 Tesla superconducting magnet. All MS/MS experiments were performed by alternating between MS and MS/MS scans throughout the chromatographic run. Isolation of the precursor ions for MS/MS was carried out in the linear ion trap with a fixed isolation window of 4  $m/z$ . Collision-induced dissociation (CID) experiments were performed entirely within the linear ion trap using helium as a collision gas and an optimised normalised collision energy level of 25%. MS Data were recorded using the acquisition software Xcalibur version 2.0.7 (ThermoFisher Corp, Bremen, Germany) and processed using the embedded program Qual Browser. Further processing and preparation of figures was done using the XCMS package<sup>2</sup> in the the R Statistical Programming Environment (version 2.13.2).<sup>3</sup>

## Blank Runs

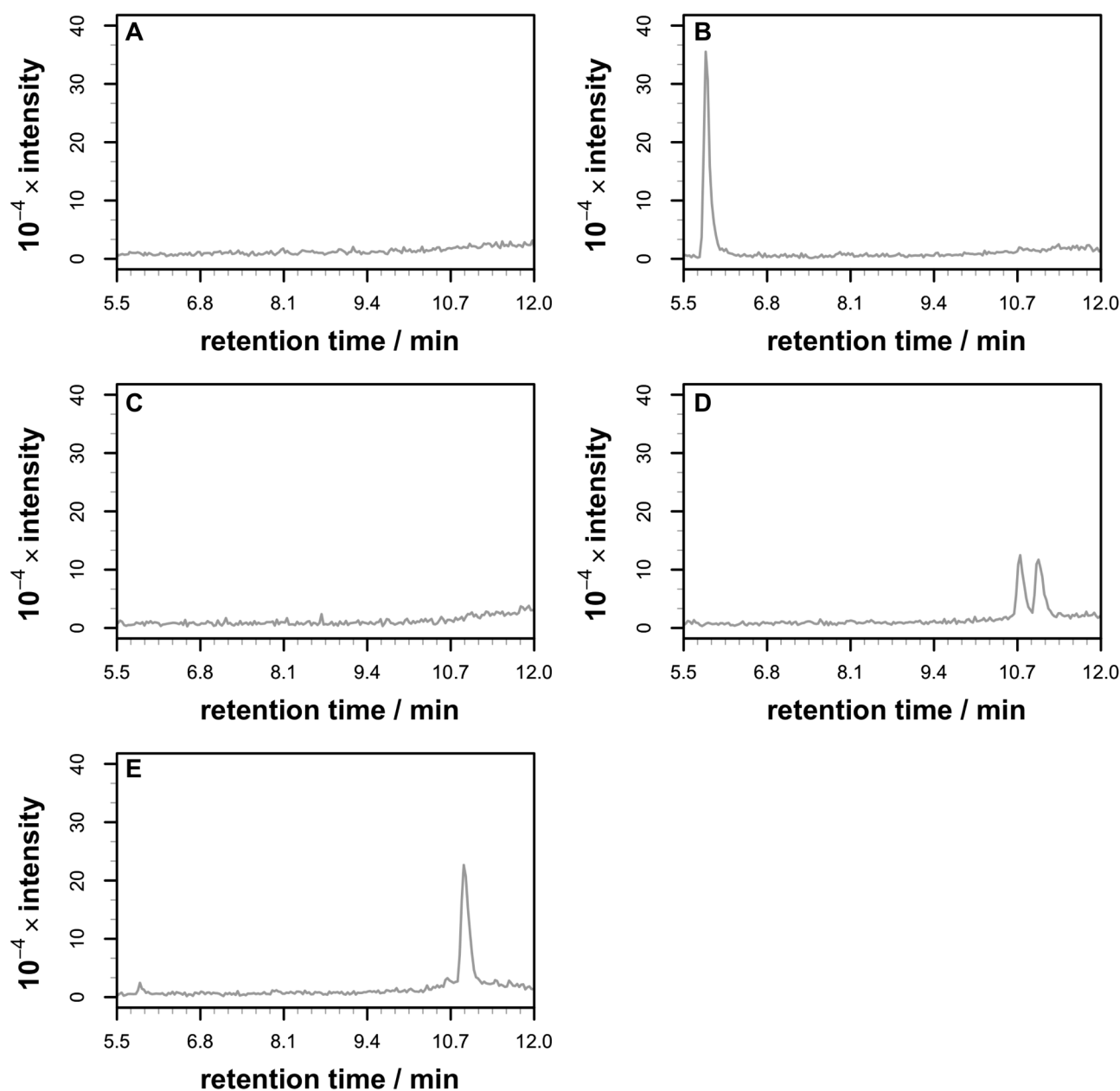


Fig. S1 LC chromatograms from blank runs, plotted as absolute intensity. (A) buffer only; (B) melittin only (no liposomes); (C) DOPC/DMPG liposomes in buffer after 4 h; (D) POPC liposomes, after 52 h; (E) DOPC/DMPG liposomes, after 52 h.

The only notable feature is the appearance of *lyso*-PCs in all samples after 2-3 days. Note that the ion currents for the *lyso*-PCs in the absence of melittin (Fig. S1D, Fig. S1E) are two orders of magnitude lower than those found in the presence of melittin (Fig. 1, main paper). Intensities for *lyso*-PCs were not used for quantification of the extent of reaction.

## Data Filtering

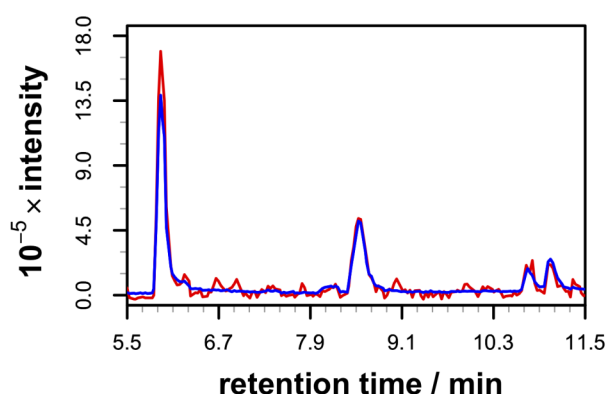


Fig. S2 Total ion current (red) and filtered ion current (blue) for POPC/melittin after 52 h, plotted as absolute intensity.

5 For the figures in the main paper, ion current data were filtered by combining the extracted ion currents (EICs) for all of the charge states of melittin, acylated melittin and *lyso*-PCs. This gave improvements in signal-to-noise ratio. Fig. S2 demonstrates that the combined EICs recapture the total ion  
 10 current (TIC) for the peaks in the chromatogram (*i.e.* data are not being lost during filtering).

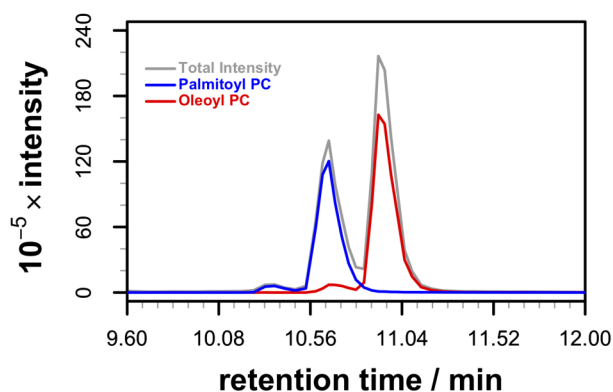
Double Peaks for *lyso*-PCs

Fig. S3 *lyso*-PC section of the LC chromatogram from POPC/melittin  
 15 after 52 h showing the TIC in this region and the EICs for both *lyso*-PCs, plotted as absolute intensities.

Each *lyso*-PC gave rise to two peaks in the chromatogram, one for the 1-acyl, and one for the 2-acyl. The intensity difference between the *lyso*-PC peak and the total intensity is due to  
 20 doubly acylated melittin.

## Peak Areas: Ion Current vs PDA

Table S1 Peak areas from the photodiode array detector and TIC chromatograms (see Fig. 1, main text).

	Peak Area (% of Total) <sup>a</sup>		Peak Area (% of Acyl Melittin) <sup>a</sup>	
	PDA	Ion Current	PDA	Ion Current
Melittin (peak i)	81	67	-	-
N-acyl (peak vi)	9	23	47	69
K23-acyl (peak v)	5	6	24	18
K7-acyl (peak iv)	1	1	3	5
K21-acyl (peak iii)	3	2	20	5
S18-acyl (peak ii)	1	1	6	4

<sup>a</sup> Peak areas were determined by fitting of an exponentially modified Gaussian function to the data.

## Additional MS Data (Melittin + POPC)

Full spectra for main peaks

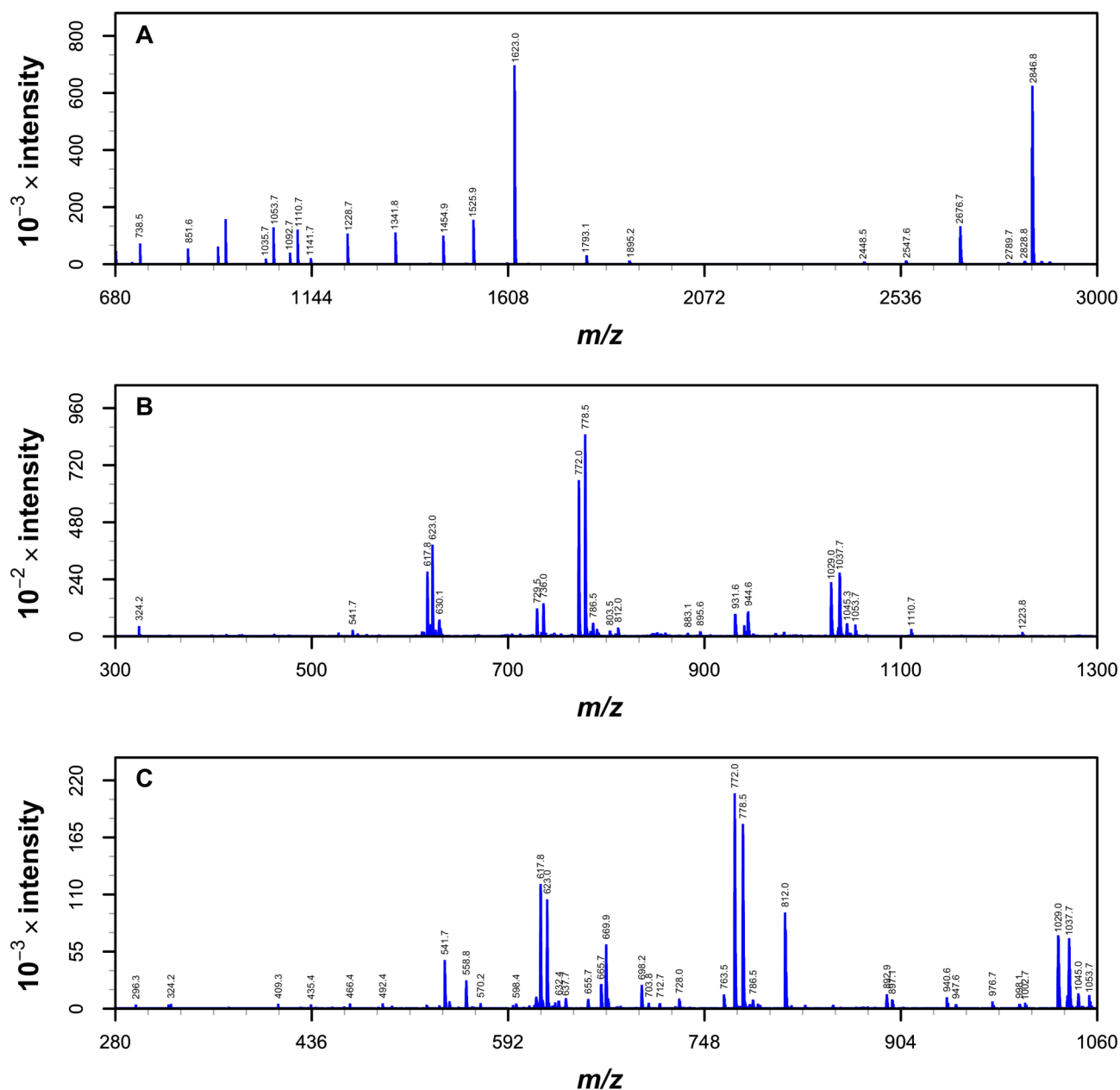


**Fig. S4** Full MS spectra. MS spectra (absolute intensities) summed over peak i (A), peak v (B) and peak vi (C) of the LC trace in Fig. 1 (main paper). (B) and (C) are full-scan versions of Fig. 2(A) and Fig. 2(B) of the main paper; (A) is deconvoluted to  $[M + H]^+$ . Peak assignments are presented below in Tables S2-S4.

**Table S2** Assignments for ions in the MS spectrum of peak i from the LC-MS trace of POPC/melittin (Fig. 1, main paper). These are the assignments for Fig. S4(A) and correspond to melittin.

ion <sup>a</sup>	Obs. <i>m/z</i>	<i>z</i>	sequence
[Mel + H] <sup>+</sup>	2845.8	1	
b <sub>26</sub> or [Mel - H <sub>2</sub> O] <sup>+</sup>	2827.8	1	
y <sub>25</sub>	2788.7	1	IGAVLKVLTTGLPALISWIKRKRQQ-NH <sub>2</sub>
y <sub>24</sub>	2675.7	1	GAVLKVLTTGLPALISWIKRKRQQ-NH <sub>2</sub>
y <sub>23</sub>	2547.6	1	AVLKVLTTGLPALISWIKRKRQQ-NH <sub>2</sub>
y <sub>22</sub>	2448.5	1	VLKVLTTGLPALISWIKRKRQQ-NH <sub>2</sub>
y <sub>16</sub>	1894.2	1	TGLPALISWIKRKRQQ-NH <sub>2</sub>
y <sub>15</sub>	1793.1	1	GLPALISWIKRKRQQ-NH <sub>2</sub>
y <sub>13</sub>	1623.0	1	PALISWIKRKRQQ-NH <sub>2</sub>
y <sub>12</sub>	1525.9	1	ALISWIKRKRQQ-NH <sub>2</sub>
y <sub>11</sub>	1454.9	1	LISWIKRKRQQ-NH <sub>2</sub>
y <sub>10</sub>	1341.8	1	ISWIKRKRQQ-NH <sub>2</sub>
y <sub>9</sub>	1228.7	1	SWIKRKRQQ-NH <sub>2</sub>
y <sub>8</sub>	1141.7	1	WIKRKRQQ-NH <sub>2</sub>
b <sub>12</sub>	1110.7	1	GIGAVLKVLTTG
b <sub>12</sub> -H <sub>2</sub> O	1092.7	1	GIGAVLKVLTTG
b <sub>11</sub>	1053.7	1	GIGAVLKVLTT
b <sub>11</sub> -H <sub>2</sub> O	1035.7	1	GIGAVLKVLTT
b <sub>9</sub>	851.6	1	GIGAVLKVL
b <sub>8</sub>	738.5	1	GIGAVLKV

<sup>a</sup> Key: Mel, melittin

5

**Table S3** Assignments for ions in the MS spectrum of peak v from the LC-MS trace of POPC/melittin (Fig. 1, main paper). These are the assignments for Fig. S4(B) and correspond to K23-acylated melittin.

ion <sup>a</sup>	Obs. <i>m/z</i>	Calc. <i>m/z</i>	<i>z</i>	sequence <sup>a</sup>
b <sub>13</sub>	1223.77	1223.77	1	GIGAVLKVLTTGL
b <sub>12</sub>	1110.69	1110.69	1	GIGAVLKVLTTG
[(Mel + Ol - H) + 3H] <sup>3+</sup>	1037.34	1037.34	3	
[(Mel + Pal - H) + 3H] <sup>3+</sup>	1028.67	1028.67	3	
b <sub>11</sub>	1053.67	1053.67	1	GIGAVLKVLTT
y <sub>13</sub>	944.13	944.12	2	PALISWIKRKRQQ-NH <sub>2</sub> [1×Ol]
y <sub>13</sub>	931.12	931.11	2	PALISWIKRKRQQ-NH <sub>2</sub> [1×Pal]
y <sub>12</sub>	895.60	895.60	2	ALISWIKRKRQQ-NH <sub>2</sub> [1×Ol]
y <sub>12</sub>	882.59	882.59	2	ALISWIKRKRQQ-NH <sub>2</sub> [1×Pal]
y <sub>10</sub>	803.54	803.54	2	ISWIKRKRQQ-NH <sub>2</sub> [1×Ol]
[(Mel + Ol - H) + 4H] <sup>4+</sup>	778.26	778.26	4	
[(Mel + Pal - H) + 4H] <sup>4+</sup>	771.75	771.75	4	
y <sub>24</sub>	735.73	735.73	4	GAVLKVLTTGLPA LISWIKRKRQQ-NH <sub>2</sub> [1×Ol]
y <sub>24</sub>	729.23	729.23	4	GAVLKVLTTGLPA LISWIKRKRQQ-NH <sub>2</sub> [1×Pal]
y <sub>13</sub>	629.75	629.75	3	PALISWIKRKRQQ-NH <sub>2</sub> [1×Ol]
[(Mel + Ol - H) + 5H] <sup>5+</sup>	622.81	622.81	5	
[(Mel + Pal - H) + 5H] <sup>5+</sup>	617.60	617.60	5	

<sup>a</sup> Key: Mel, melittin; Ol, oleoyl; Pal, palmitoyl

10

**Table S4** Assignments for ions in the MS spectrum of peak vi from the LC-MS trace of POPC/melittin (Fig. 1, main paper). These are the assignments for Fig. S4(C) and correspond to N-acylated melittin.

ion <sup>a</sup>	Obs. <i>m/z</i>	Calc. <i>m/z</i>	<i>z</i>	sequence <sup>a</sup>
[(Mel + Ol - H) + 2H] <sup>2+</sup>	1555.51	1555.51	2	
[(Mel + Pal - H) + 2H] <sup>2+</sup>	1542.50	1542.50	2	
[(Mel + Ol - H) + 2H + Na] <sup>3+</sup>	1044.67	1044.67	3	
[(Mel + Ol - H) + 2H + Na] <sup>3+</sup>	1036.00	1036.00	3	
[(Mel + Ol - H) + 3H] <sup>3+</sup>	1037.34	1037.34	3	
[(Mel + Pal - H) + 3H] <sup>3+</sup>	1028.67	1028.67	3	
b <sub>8</sub>	1002.73	1002.73	1	GIGAVLKV [1×Ol]
y <sub>17</sub>	998.10	998.10	2	TTGLPALISWIKRKRQQ-NH <sub>2</sub>
b <sub>8</sub>	976.72	976.72	1	GIGAVLKV [1×Pal]
y <sub>16</sub>	947.58	947.58	2	TGLPALISWIKRKRQQ-NH <sub>2</sub>
y <sub>15</sub>	897.06	897.06	2	GLPALISWIKRKRQQ-NH <sub>2</sub>
[(Mel + Ol - H) + 4H] <sup>4+</sup>	778.25	778.25	4	
[(Mel + Pal - H) + 4H] <sup>4+</sup>	771.75	771.75	4	
y <sub>12</sub>	763.48	763.48	2	ALISWIKRKRQQ-NH <sub>2</sub>
y <sub>11</sub>	727.96	727.96	2	LISWIKRKRQQ-NH <sub>2</sub>
y <sub>18</sub>	703.43	703.43	3	LTGLPALISWIKRKRQQ-NH <sub>2</sub>
y <sub>25</sub>	697.94	697.94	4	IGAVLKVLTTGLPALISWIKRKRQQ-NH <sub>2</sub>
y <sub>24</sub>	669.65	669.65	4	GAVLKVLTTGLPALISWIKRKRQQ-NH <sub>2</sub>
y <sub>17</sub>	665.74	665.74	3	TTGLPALISWIKRKRQQ-NH <sub>2</sub>
y <sub>23</sub>	655.42	655.42	4	AVLKVLTTGLPALISWIKRKRQQ-NH <sub>2</sub>
y <sub>22</sub>	637.66	637.66	4	VLKVLTTGLPALISWIKRKRQQ-NH <sub>2</sub>
y <sub>16</sub>	632.06	632.06	3	TGLPALISWIKRKRQQ-NH <sub>2</sub>
[(Mel + Ol - H) + 5H] <sup>5+</sup>	622.81	622.81	5	
[(Mel + Pal - H) + 5H] <sup>5+</sup>	617.60	617.60	5	
y <sub>15</sub>	598.37	598.37	3	GLPALISWIKRKRQQ-NH <sub>2</sub>
y <sub>25</sub>	558.55	558.55	5	IGAVLKVLTTGLPALISWIKRKRQQ-NH <sub>2</sub>
y <sub>13</sub>	541.67	541.67	3	PALISWIKRKRQQ-NH <sub>2</sub>
b <sub>3</sub>	492.38	492.38	1	GIG [1×Ol]
b <sub>3</sub>	466.36	466.36	1	GIG [1×Pal]
b <sub>2</sub>	435.36	435.36	1	GI [1×Ol]
b <sub>2</sub>	409.34	409.34	1	GI [1×Pal]
b <sub>1</sub>	322.27	322.27	1	G [1×Ol]
b <sub>1</sub>	296.26	296.26	1	G [1×Pal]

<sup>a</sup> Key: Ol, oleoyl; Pal, palmitoyl

15

## N-oleoyl melittin

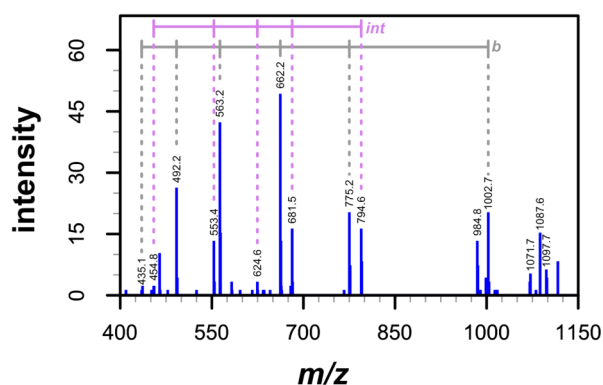


**Fig. S5** MS<sup>3</sup> spectrum (absolute intensity) for N-oleoyl melittin in peak vi of the POPC chromatogram (Fig. 1 in the main paper). MS/MS precursor ion  $m/z$  778; MS<sup>3</sup> precursor ion  $m/z$  1115.5. This is the oleoyl equivalent of Fig. 3C in the main paper)

**Table S5** Assignments for ions in the MS<sup>3</sup> spectrum of N-oleoyl melittin (Fig. S5)

ion	#	Obs. $m/z$	$z$	sequence <sup>a</sup>
$b_8$	8	1002.7	1	GIGAVLKV [1×OI]
$b_6$	6	775.2	1	GIGAVL [1×OI]
$b_5$	5	662.2	1	GIGAV [1×OI]
$b_4$	4	563.3	1	GIGA [1×OI]
$b_3$	3	492.2	1	GIG [1×OI]
$b_2$	2	435.1	1	GI [1×OI]
$b_8-H_2O$	8	984.8	1	GIGAVLKV [1×OI]
$b_9-H_2O$	9	1097.7	1	GIGAVLKVL [1×OI]
$b_9-CO$	9	1087.6	1	GIGAVLKVL [1×OI]
$b_9-CO_2$	9	1071.7	1	GIGAVLKVL [1×OI]
int	-	455.5	1	LKVL <sup>‡</sup>
int	-	553.4	1	VLKVL <sup>‡</sup>
int	-	624.6	1	AVLKVL <sup>‡</sup>
int	-	681.5	1	GAVLKVL <sup>‡</sup>
int	-	794.6	1	IGAVLKVL <sup>‡</sup>

<sup>a</sup> Key: M, melittin; OI, Oleoyl; <sup>‡</sup> this is the closest match for this ion series, although the error between the observed and calculated  $m/z$  is 1 unit. This may be due to an uncharacterised rearrangement occurring due to the proximity of these residues to the oleoyl modification.

## MS/MS data

**Table S6** Assignments for ions in the MS/MS spectrum of peak vi (Fig. 1, main paper), precursor ion  $m/z$  772.0 (assignments for Fig. 3(A) in the main paper).

ion	Obs. $m/z$	$z$	sequence <sup>a</sup>
y <sub>12</sub>	763.2	2	ALISWIKRKRQQ-NH <sub>2</sub>
y <sub>13</sub>	812.8	2	PALISWIKRKRQQ-NH <sub>2</sub>
y <sub>14</sub>	868.8	2	LPALISWIKRKRQQ-NH <sub>2</sub>
y <sub>15</sub>	897.3	2	GLPALISWIKRKRQQ-NH <sub>2</sub>
y <sub>16</sub>	947.9	2	TGLPALISWIKRKRQQ-NH <sub>2</sub>
y <sub>17</sub>	998.5	2	TTGLPALISWIKRKRQQ-NH <sub>2</sub>
y <sub>13</sub>	542.1	3	PALISWIKRKRQQ-NH <sub>2</sub>
y <sub>16</sub>	632.4	3	TGLPALISWIKRKRQQ-NH <sub>2</sub>
y <sub>17</sub>	666.6	3	TTGLPALISWIKRKRQQ-NH <sub>2</sub>
y <sub>21</sub>	817.3	3	LKVLTTGLPALISWIKRKRQQ-NH <sub>2</sub>
b <sub>2</sub>	409.0	1	GI [1×Pal]
b <sub>3</sub>	466.2	1	GIG [1×Pal]
b <sub>4</sub>	537.2	1	GIGA [1×Pal]
b <sub>5</sub>	636.3	1	GIGAV [1×Pal]
b <sub>6</sub>	749.3	1	GIGAVL [1×Pal]
b <sub>7</sub>	877.3	1	GIGAVLK [1×Pal]
b <sub>8</sub>	976.6	1	GIGAVLKV [1×Pal]
b <sub>9</sub>	1089.6	1	GIGAVLKVL [1×Pal]
b <sub>10</sub>	1190.6	1	GIGAVLKVLT [1×Pal]
b <sub>12</sub>	1348.7	1	GIGAVLKVLTTG [1×Pal]
b <sub>13</sub>	1461.8	1	GIGAVLKVLTTGL [1×Pal]
b <sub>7</sub>	439.4	2	GIGAVLK [1×Pal]
b <sub>8</sub>	488.9	2	GIGAVLKV [1×Pal]
b <sub>10</sub>	596.1	2	GIGAVLKVLT [1×Pal]
b <sub>13</sub>	730.8	2	GIGAVLKVLTTGL [1×Pal]
b <sub>13</sub>	488.9	3	GIGAVLKVLTTGL [1×Pal]
b <sub>18</sub>	972.4	2	GIGAVLKVLTTGLPALIS [1×Pal]
b <sub>22</sub>	844.6	3	GIGAVLKVLTTGLPALISWIKR [1×Pal]
b <sub>22</sub>	632.4	4	GIGAVLKVLTTGLPALISWIKR [1×Pal]
b <sub>24</sub>	703.7	4	GIGAVLKVLTTGLPALISWIKRKR [1×Pal]
b <sub>25</sub>	980.7	3	GIGAVLKVLTTGLPALISWIKRKRQ [1×Pal]

<sup>a</sup> Key: Pal, palmitoyl**Table S7** Assignments for ions in the MS/MS spectrum of peak v, precursor ion  $m/z$  778.5 (assignments for Fig. 3(B) in the main paper).

ion	Obs. $m/z$	$z$	sequence <sup>a</sup>
y <sub>8</sub>	703.8	2	WIKRKRQQ-NH <sub>2</sub> [1×Ol]
y <sub>9</sub>	747.2	2	SWIKRKRQQ-NH <sub>2</sub> [1×Ol]
y <sub>10</sub>	803.8	2	ISWIKRKRQQ-NH <sub>2</sub> [1×Ol]
y <sub>11</sub>	860.4	2	LISWIKRKRQQ-NH <sub>2</sub> [1×Ol]
y <sub>12</sub>	895.9	2	ALISWIKRKRQQ-NH <sub>2</sub> [1×Ol]
y <sub>13</sub>	944.4	2	PALISWIKRKRQQ-NH <sub>2</sub> [1×Ol]
y <sub>14</sub>	1000.9	2	LPALISWIKRKRQQ-NH <sub>2</sub> [1×Ol]
y <sub>15</sub>	1029.4	2	GLPALISWIKRKRQQ-NH <sub>2</sub> [1×Ol]
y <sub>16</sub>	1080.0	2	TGLPALISWIKRKRQQ-NH <sub>2</sub> [1×Ol]
y <sub>17</sub>	1130.5	2	TTGLPALISWIKRKRQQ-NH <sub>2</sub> [1×Ol]
y <sub>10</sub>	538.0	3	LSWIKRKRQQ-NH <sub>2</sub> [1×Ol]
y <sub>13</sub>	630.3	3	PALISWIKRKRQQ-NH <sub>2</sub> [1×Ol]
y <sub>14</sub>	667.9	3	LPALISWIKRKRQQ-NH <sub>2</sub> [1×Ol]
y <sub>16</sub>	720.4	3	TGLPALISWIKRKRQQ-NH <sub>2</sub> [1×Ol]
y <sub>17</sub>	754.0	3	TTGLPALISWIKRKRQQ-NH <sub>2</sub> [1×Ol]
y <sub>20</sub>	867.6	3	KVLTTGLPALISWIKRKRQQ-NH <sub>2</sub> [1×Ol]
y <sub>21</sub>	905.3	3	LKVLTTGLPALISWIKRKRQQ-NH <sub>2</sub> [1×Ol]
y <sub>22</sub>	938.4	3	VLKVLTTGLPALISWIKRKRQQ-NH <sub>2</sub> [1×Ol]
y <sub>23</sub>	962.2	3	AVLKVLTTGLPALISWIKRKRQQ-NH <sub>2</sub> [1×Ol]
y <sub>24</sub>	981.2	3	GAVLKVLTTGLPALISWIKRKRQQ-NH <sub>2</sub> [1×Ol]
y <sub>18</sub>	594.6	4	LTTGLPALISWIKRKRQQ-NH <sub>2</sub> [1×Ol]
y <sub>24</sub>	736.1	4	GAVLKVLTTGLPALISWIKRKRQQ-NH <sub>2</sub> [1×Ol]
b <sub>6</sub>	511.2	1	GIGAVL
b <sub>7</sub>	639.3	1	GIGAVLK
b <sub>8</sub>	738.5	1	GIGAVLKV
b <sub>9</sub>	851.6	1	GIGAVLKVL
b <sub>11</sub>	1053.5	1	GIGAVLKVLTT
b <sub>12</sub>	1110.6	1	GIGAVLKVLTTG
b <sub>13</sub>	1223.6	1	GIGAVLKVLTTGL

<sup>a</sup> Key: Ol, oleoyl

10

## Spectra for minor monoacylated products

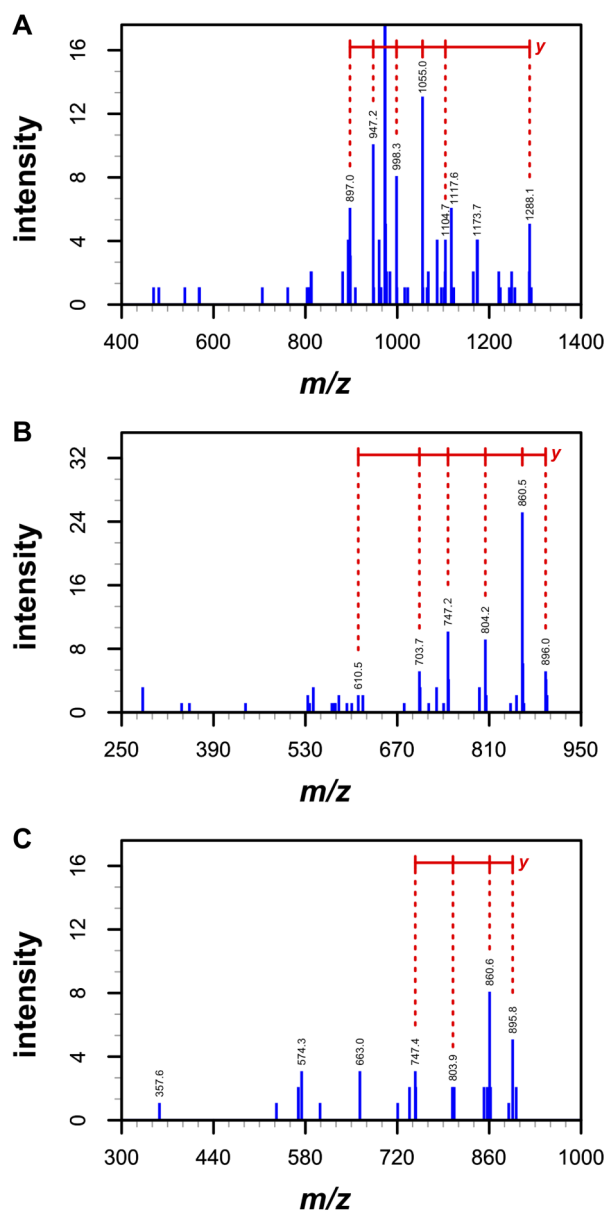


Fig. S6 MS spectra ( $MS^3$ ) from the centre (maximum absolute intensity) of each of peaks ii, iii and iv (Fig. 1, main article). (A): peak iv, MS/MS precursor ion  $m/z$  772,  $MS^3$  precursor ion  $m/z$  972; (B): peak iii, MS/MS precursor ion  $m/z$  778,  $MS^3$  precursor ion  $m/z$  630.2; (C): peak ii, MS/MS precursor ion  $m/z$  778,  $MS^3$  precursor ion  $m/z$  630.2.

Table S8 Identity of the  $MS^3$  precursor ion with  $m/z$  972 (Fig. 5(A), Fig. S6(A), Table S9).

ion <sup>b</sup>	Obs. $m/z$	Calc. $m/z$	$z$	sequence <sup>a</sup>
y	972.8	972.6	3	GAVLKVLTGLPALISWIKRKRQQ-NH <sub>2</sub> [1×Pal]

<sup>a</sup> Key: Pal, palmitoyl; <sup>b</sup> this is the precursor ion for peaks ii–v in Fig 5(A) (main paper) and Table S9 (but *not* Tables S10 and S11)

Table S9 Assignments for ions in the  $MS^3$  spectrum from the centre (maximum intensity) of peak iv (Fig. 1, main article). MS/MS precursor ion  $m/z$  772,  $MS^3$  precursor ion  $m/z$  972; corresponds to Fig. S6(A).

ion <sup>a</sup>	Obs. $m/z$	$z$	sequence <sup>a</sup>
y <sub>20</sub>	1288.1	2	KVLTGLPALISWIKRKRQQ-NH <sub>2</sub> [1×Pal]
y <sub>19</sub>	1104.7	2	VLTGLPALISWIKRKRQQ-NH <sub>2</sub>
y <sub>18</sub>	1055.0	2	LTTGLPALISWIKRKRQQ-NH <sub>2</sub>
y <sub>17</sub>	998.3	2	TTGLPALISWIKRKRQQ-NH <sub>2</sub>
y <sub>16</sub>	947.2	2	TGLPALISWIKRKRQQ-NH <sub>2</sub>
y <sub>15</sub>	897.0	2	GLPALISWIKRKRQQ-NH <sub>2</sub>

<sup>a</sup> Key: Pal, palmitoyl

Table S10 Assignments for ions in the  $MS^3$  spectrum from the centre (maximum intensity) of peak iii (Fig. 1, main article). MS/MS precursor ion  $m/z$  778,  $MS^3$  precursor ion  $m/z$  630.2; corresponds to Fig. S6(B).

ion <sup>a</sup>	Obs. $m/z$	$z$	sequence <sup>a</sup>
y <sub>7</sub>	610.6	2	IKRKRQQ-NH <sub>2</sub> [1×OI]
y <sub>8</sub>	703.8	2	WIKRKRQQ-NH <sub>2</sub> [1×OI]
y <sub>9</sub>	747.2	2	SWIKRKRQQ-NH <sub>2</sub> [1×OI]
y <sub>10</sub>	803.8	2	ISWIKRKRQQ-NH <sub>2</sub> [1×OI]
y <sub>11</sub>	860.4	2	LISWIKRKRQQ-NH <sub>2</sub> [1×OI]
y <sub>12</sub>	895.8	2	ALISWIKRKRQQ-NH <sub>2</sub> [1×OI]

int 282.1 1 PAL

<sup>a</sup> Key: OI, oleoyl; int, internal

Table S11 Assignments for ions in the  $MS^3$  spectrum from the centre (maximum intensity) of peak ii (Fig. 1, main article). MS/MS precursor ion  $m/z$  778,  $MS^3$  precursor ion  $m/z$  630.2; corresponds to Fig. S6(C).

ion <sup>a</sup>	Obs. $m/z$	$z$	sequence <sup>a</sup>
y <sub>9</sub>	747.4	2	SWIKRKRQQ-NH <sub>2</sub> [1×OI]
y <sub>10</sub>	803.9	2	ISWIKRKRQQ-NH <sub>2</sub> [1×OI]
y <sub>11</sub>	860.6	2	LISWIKRKRQQ-NH <sub>2</sub> [1×OI]
y <sub>12</sub>	895.8	2	ALISWIKRKRQQ-NH <sub>2</sub> [1×OI]

y<sub>5</sub> 357.6 2 RKRQQ-NH<sub>2</sub>

<sup>a</sup> Key: OI, oleoyl

## Doubly acylated melittin

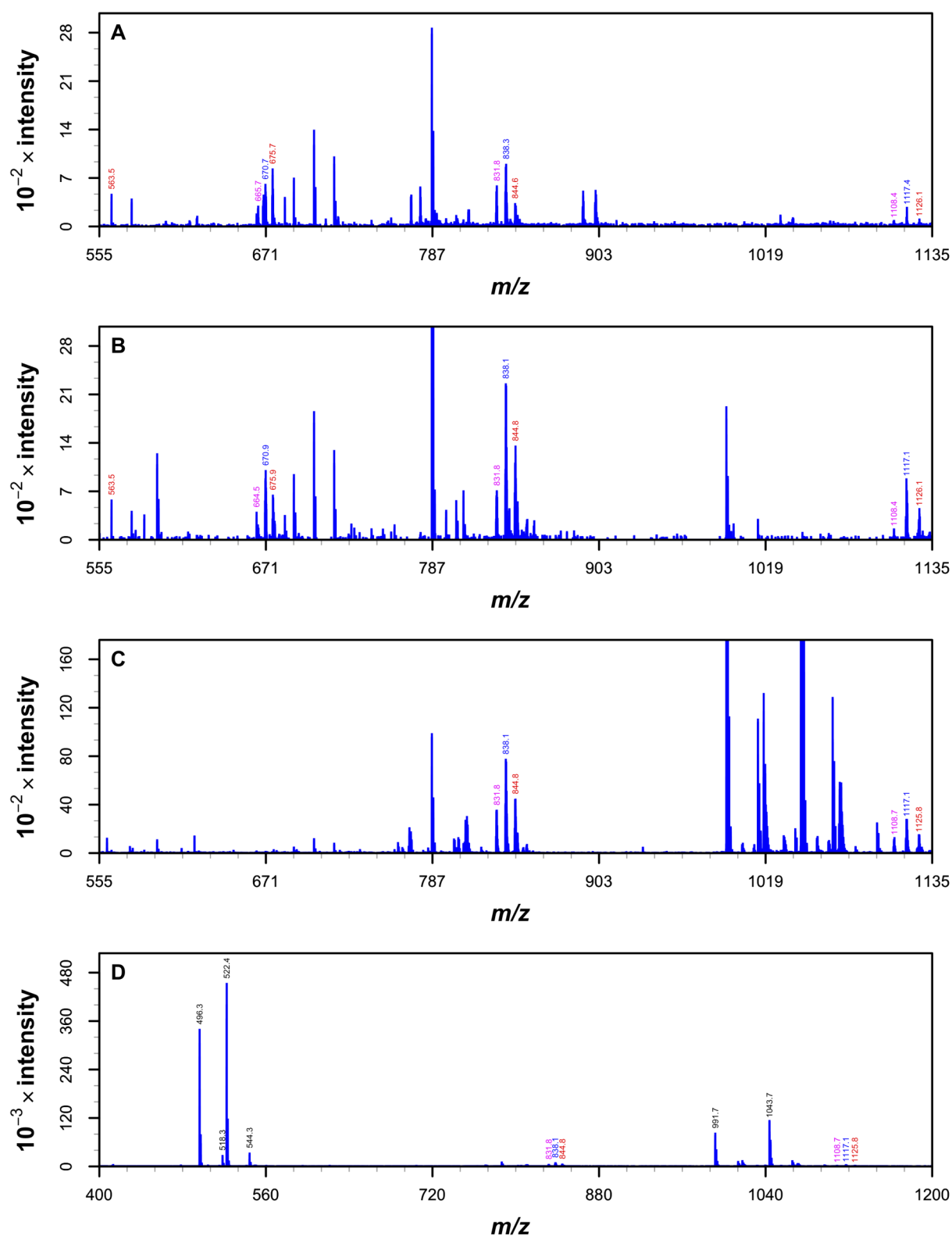


Fig. S7 MS spectra (absolute intensities) for doubly-acylated melittin. (A), RT range 9.3–9.7; (B), RT range 10.0–10.4; (C), RT range 10.4–11.4 (scaled to show doubly-acylated peaks); (D), RT range 10.4–11.4 (full y-range; main peaks are both *lyso*-PCs, plus their sodium adducts, and their proton dimers, see Table S12).

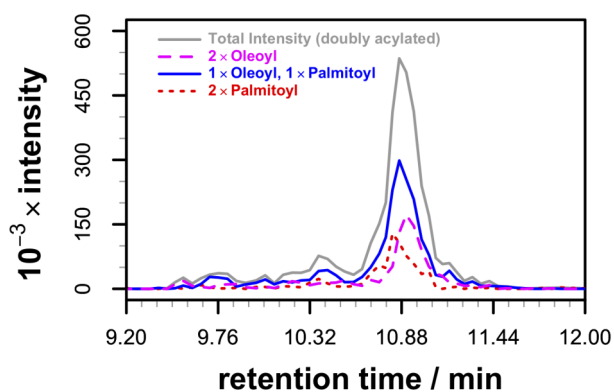
5

**Table S12** Assignments for doubly acylated melittin (Fig. S7). Other data are given only for the main peaks in Fig. S7(A)–(D).

ion <sup>a</sup>	Obs. <i>m/z</i>	Calc. <i>m/z</i>	<i>z</i>
[(Mel + 2Ol – 2H) + 3H] <sup>3+</sup>	1125.42275	1125.42221	3
[(Mel + Ol + Pal – 2H) + 3H] <sup>3+</sup>	1115.75236	1116.75033	3
[(Mel + 2Pal – 2H) + 3H] <sup>3+</sup>	1108.08106	1108.07844	3
[(Mel + 2Ol – 2H) + 4H] <sup>4+</sup>	844.32010	844.31848	4
[(Mel + Ol + Pal – 2H) + 4H] <sup>4+</sup>	837.81633	837.81457	4
[(Mel + 2Pal – 2H) + 4H] <sup>4+</sup>	831.31244	831.31065	4
[(Mel + 2Ol – 2H) + 5H] <sup>5+</sup>	675.65762	675.65624	5
[(Mel + Ol + Pal – 2H) + 5H] <sup>5+</sup>	670.45455	670.45311	5
[(Mel + 2Ol – 2H) + 5H] <sup>5+</sup>	665.24956	665.24998	5
[(2 × mono-Oleoyl-PC) + H] <sup>+</sup>	1043.70454	1043.70356	1
[(2 × mono-Palmitoyl-PC) + H] <sup>+</sup>	991.67352	991.67226	1
[mono-Oleoyl-PC + Na] <sup>+</sup>	544.33856	544.33736	1
[mono-Oleoyl-PC + H] <sup>+</sup>	522.35577	522.35542	1
[mono-Palmitoyl-PC + Na] <sup>+</sup>	518.32273	518.32171	1
[mono-Palmitoyl-PC + H] <sup>+</sup>	496.34007	496.33977	1

<sup>a</sup> Key: Mel, melittin; Ol, oleoyl; Pal, palmitoyl; PC, phosphocholine. All observed masses are accurate to within 3 ppm.

5

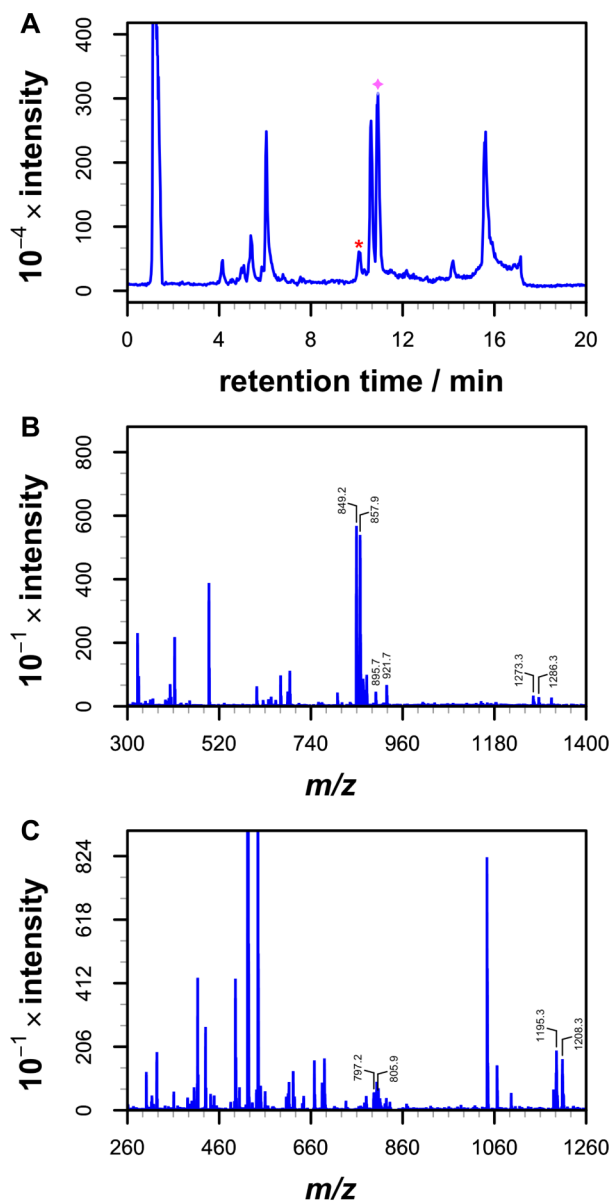
**Fig. S8** Total and extracted ion intensities (absolute values) for doubly acylated melittin in the reaction with POPC after 52 h.

## 10 Tryptic digests of acylated melittin

Fig. S9(B) shows the mass spectrum of the most abundant lipidated peak in the digest profile, matching the sequence GIGAVLKVLTTGLPALISWIKR; *m/z* 849.2/1273.3 and 857.9/1286.3 correspond to [M + 3H]<sup>3+</sup>/[M + 2H]<sup>2+</sup> for the palmitoylated and oleoylated peptides respectively. In addition, two ions are detectable with *m/z* 895.7 and 921.7 that correspond respectively to [M + H]<sup>+</sup> for the sequence GIGAVLK + palmitoyl and GIGAVLK + oleoyl. Fig. S9(C) shows the only other product detectable,

GIGAVLKVLTTGLPALISWIK; *m/z* 797.2/1195.3 and 805.9/1208.3 correspond to [M + 3H]<sup>3+</sup>/[M + 2H]<sup>2+</sup> for the palmitoylated and oleoylated peptides respectively. These experiments were of necessity conducted with an excess of unreacted peptide present in the mixture, with the consequence that the detection of unmodified fragments could not be used to locate the positions of acylation. In addition, extensive digestion was not observed for the lipidated peptide,

rendering the results from tryptic digests inconclusive. Nevertheless, the most abundant lipidated peptides (Fig S9(B) and (C)) are consistent with N-terminal acylation as a major product.

**Fig. S9** (A) LC trace following trypsin digestion of a melittin/OPPC sample after 3 days incubation. The peaks indicated by an asterisk and a diamond contain acylated products (although the main component of the peak indicated with a diamond is 1-oleoyl-PC). (B) mass spectrum from the peak indicated by an asterisk; (C) mass spectrum of the peak indicated by a diamond. LC conditions as Fig. 1 (main article).

40

## Reaction with DOPC/DPPS

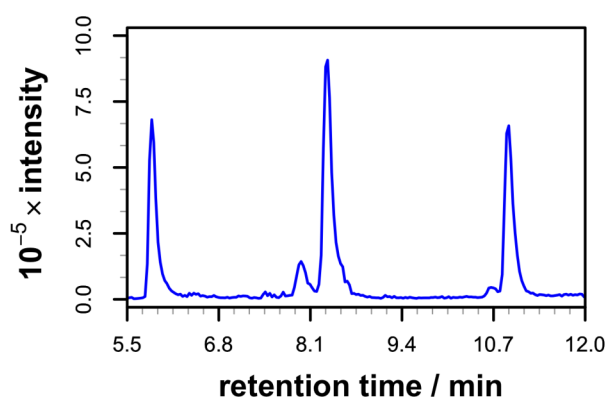


**Fig. S10** TIC (absolute intensity) for the incubation of melittin (0.25 mM) with DOPC/DPPS (45  $\mu$ M) at 37  $^{\circ}$ C in 10 mM  $\text{NaHCO}_3$ /90 mM NaCl, after 53 h. Separation was performed using an Xbridge C18, column (Waters, UK), with a linear gradient of 95%  $\text{H}_2\text{O}$ /5% MeCN to 5%  $\text{H}_2\text{O}$ /95% MeCN in 12 min.

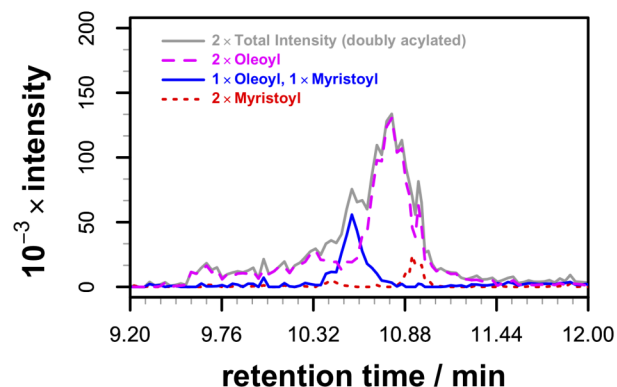


**Fig. S12** Total and extracted ion intensities (absolute values) for doubly acylated melittin in the reaction with DMPG/DOPC after 52 h.

## Reaction with DOPC/DMPG

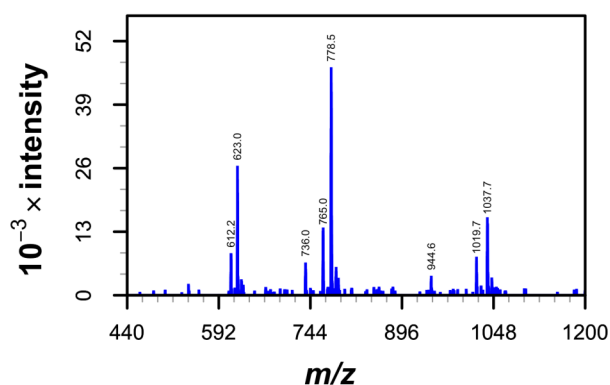


**Fig. S11** Mass spectrum from peak iii of the melittin+DMPG/DOPC LC chromatogram (Fig. 9, main paper).

**Table S13** Assignments for ions in the MS spectrum (Fig. S11, above) from peak iii of the DMPG/DOPC chromatogram (Fig. 9, main paper).

ion <sup>a</sup>	Obs. <i>m/z</i>	Calc. <i>m/z</i>	<i>z</i>	sequence <sup>a</sup>
$[(\text{Mel} + \text{Myr} - \text{H}) + 5\text{H}]^{5+}$	612.00	612.00	5	
$[(\text{Mel} + \text{Ol} - \text{H}) + 5\text{H}]^{5+}$	622.81	622.81	5	
$y_{24}$	735.73	735.73	4	GAVLKVLTTGLPA LISWIKRKRQQ- NH <sub>2</sub> [1 $\times$ Ol]
$[(\text{Mel} + \text{Myr} - \text{H}) + 4\text{H}]^{4+}$	764.75	764.75	4	
$[(\text{Mel} + \text{Ol} - \text{H}) + 4\text{H}]^{4+}$	778.26	778.26	4	
$y_{13}$	944.13	944.12	2	PALISWIKRKRQQ- NH <sub>2</sub> [1 $\times$ Ol]
$[(\text{Mel} + \text{Myr} - \text{H}) + 3\text{H}]^{3+}$	1019.32	1019.32	3	
$[(\text{Mel} + \text{Ol} - \text{H}) + 3\text{H}]^{3+}$	1037.34	1037.34	3	

<sup>a</sup> Key: Mel, melittin; Myr, myristoyl; Ol, oleoyl

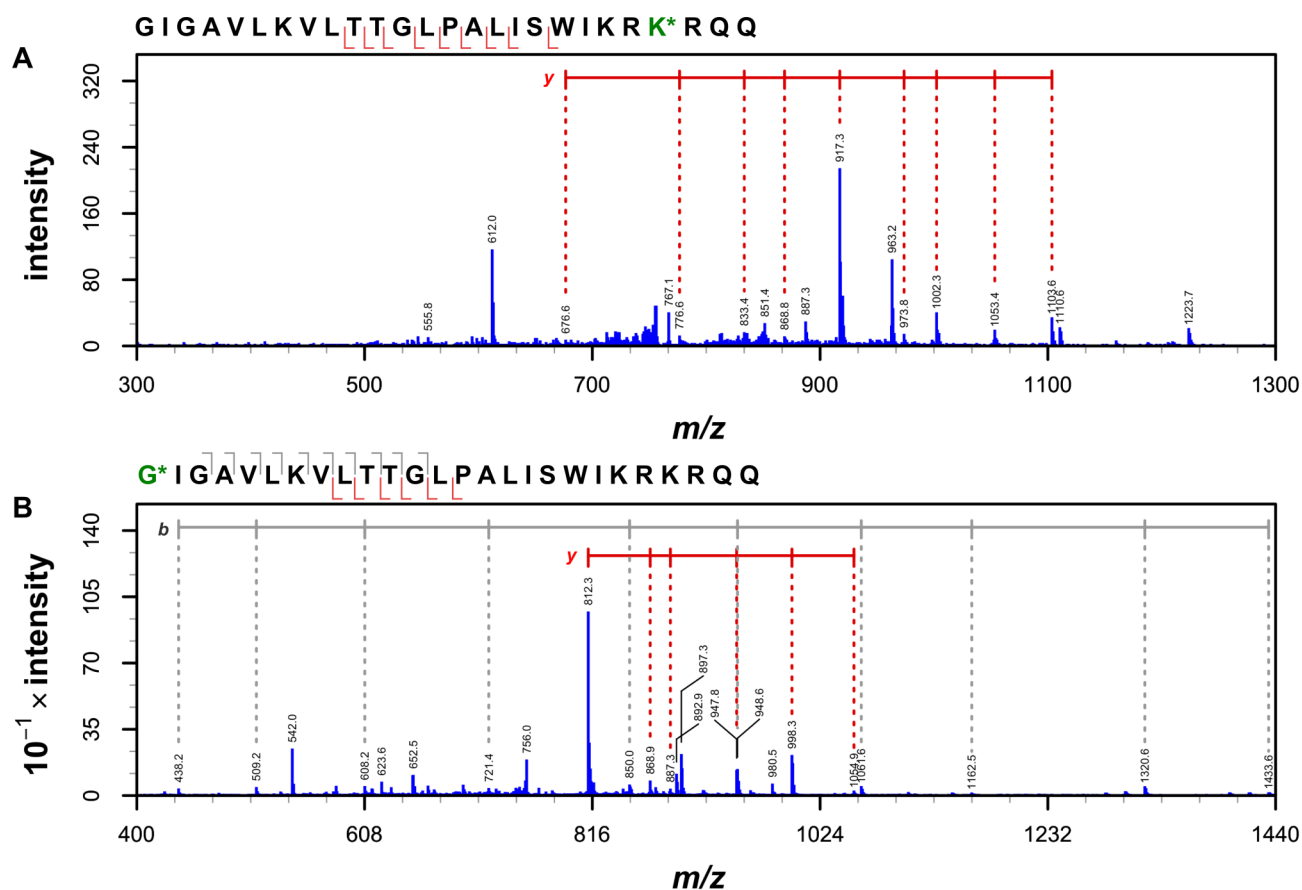


**Fig. S13** MS/MS spectra (absolute intensities) for key peaks in the LC-MS chromatogram for the reaction of melittin with DOPC/DMPG (Fig. 9, main paper): (A) peak iii, precursor ion  $m/z$  765.0; (B) peak iv, precursor ion  $m/z$  765.0. Residues (G\*, K\*) matching the site of modification are indicated by asterisks. Full assignments are given in Tables S14 and S15.

5

**Table S14** Assignments for ions in the MS/MS spectrum of peak iii in the DMPG/DOPC LC chromatogram (Fig. 9 main paper), precursor ion *m/z* 765. Assignments correspond to Fig. S13(A).

ion	Obs. <i>m/z</i>	<i>z</i>	sequence <sup>a</sup>
y <sub>8</sub>	676.6	2	WIKRKRQ-NH <sub>2</sub> [1×Myr]
y <sub>9</sub>	720.3	2	SWIKRKRQ-NH <sub>2</sub> [1×Myr]
y <sub>10</sub>	776.6	2	ISWIKRKRQ-NH <sub>2</sub> [1×Myr]
y <sub>11</sub>	833.4	2	LISWIKRKRQ-NH <sub>2</sub> [1×Myr]
y <sub>12</sub>	868.8	2	ALISWIKRKRQ-NH <sub>2</sub> [1×Myr]
y <sub>13</sub>	917.3	2	PALISWIKRKRQ-NH <sub>2</sub> [1×Myr]
y <sub>14</sub>	973.8	2	LPALISWIKRKRQ-NH <sub>2</sub> [1×Myr]
y <sub>15</sub>	1002.3	2	GLPALISWIKRKRQ-NH <sub>2</sub> [1×Myr]
y <sub>16</sub>	1053.4	2	TGLPALISWIKRKRQ-NH <sub>2</sub> [1×Myr]
y <sub>17</sub>	1103.6	2	TTGLPALISWIKRKRQ-NH <sub>2</sub> [1×Myr]
y <sub>18</sub>	1160.0	2	LTTGLPALISWIKRKRQ-NH <sub>2</sub> [1×Myr]
y <sub>24</sub>	963.2	3	GAVLKVLTGLPALISWIKRKRQ-NH <sub>2</sub> [1×Myr]
y <sub>21</sub>	887.3	3	LKVLTGLPALISWIKRKRQ-NH <sub>2</sub> [1×Myr]
y <sub>13</sub>	612.0	3	PALISWIKRKRQ-NH <sub>2</sub> [1×Myr]
y <sub>11</sub>	555.8	3	LISWIKRKRQ-NH <sub>2</sub> [1×Myr]
b <sub>9</sub>	851.4	1	GIGAVLKVL
b <sub>11</sub>	1053.4	1	GIGAVLKVLT
b <sub>12</sub>	1110.5	1	GIGAVLKVLTG
b <sub>13</sub>	1223.7	1	GIGAVLKVLTG

<sup>a</sup> Key: Myr, myristoyl

5

**Table S15** Assignments for ions in the MS/MS spectrum of peak iv in the DMPG/DOPC LC chromatogram (Fig. 9 main paper) precursor ion *m/z* 765. Assignments correspond to Fig. S13(B).

ion	Obs. <i>m/z</i>	<i>z</i>	sequence <sup>a</sup>
y <sub>9</sub>	615.2	2	SWIKRKRQ-NH <sub>2</sub>
y <sub>10</sub>	671.5	2	ISWIKRKRQ-NH <sub>2</sub>
y <sub>11</sub>	728.1	2	LISWIKRKRQ-NH <sub>2</sub>
y <sub>13</sub>	812.3	2	PALISWIKRKRQ-NH <sub>2</sub>
y <sub>14</sub>	868.9	2	LPALISWIKRKRQ-NH <sub>2</sub>
y <sub>15</sub>	897.3	2	GLPALISWIKRKRQ-NH <sub>2</sub>
y <sub>16</sub>	947.8	2	TGLPALISWIKRKRQ-NH <sub>2</sub>
y <sub>17</sub>	998.3	2	TTGLPALISWIKRKRQ-NH <sub>2</sub>
y <sub>18</sub>	1054.9	2	LTTGLPALISWIKRKRQ-NH <sub>2</sub>
y <sub>12</sub> <sup>b</sup>	509.2	3	ALISWIKRKRQ-NH <sub>2</sub>
y <sub>13</sub>	542.0	3	PALISWIKRKRQ-NH <sub>2</sub>
y <sub>14</sub>	579.5	3	LPALISWIKRKRQ-NH <sub>2</sub>
y <sub>15</sub>	598.4	3	GLPALISWIKRKRQ-NH <sub>2</sub>
y <sub>16</sub>	632.4	3	TGLPALISWIKRKRQ-NH <sub>2</sub>
y <sub>17</sub>	665.9	3	TTGLPALISWIKRKRQ-NH <sub>2</sub>
y <sub>18</sub>	703.7	3	LTTGLPALISWIKRKRQ-NH <sub>2</sub>
y <sub>20</sub>	779.4	3	KVLTGLPALISWIKRKRQ-NH <sub>2</sub>
y <sub>22</sub> <sup>b</sup>	850.0	3	VLKVLTTGLPALISWIKRKRQ-NH <sub>2</sub>
y <sub>23</sub>	873.9	3	AVLKVLTTGLPALISWIKRKRQ-NH <sub>2</sub>
y <sub>24</sub>	892.9	3	GAVLKVLTTGLPALISWIKRKRQ-NH <sub>2</sub>
y <sub>25</sub>	698.1	4	IGAVLKVLTGLPALISWIKRKRQ-NH <sub>2</sub>
b <sub>3</sub>	438.2	1	GIG [1×Myr]
b <sub>4</sub> <sup>b</sup>	509.2	1	GIGA [1×Myr]
b <sub>5</sub>	608.2	1	GIGAV [1×Myr]
b <sub>6</sub>	721.4	1	GIGAVL [1×Myr]
b <sub>7</sub> <sup>b</sup>	850.0	1	GIGAVLK [1×Myr]
b <sub>8</sub>	948.6	1	GIGAVLKV [1×Myr]
b <sub>9</sub>	1061.6	1	GIGAVLKVL [1×Myr]
b <sub>10</sub>	1162.5	1	GIGAVLKVLT [1×Myr]
b <sub>12</sub>	1320.6	1	GIGAVLKVLTG [1×Myr]
b <sub>13</sub>	1433.6	1	GIGAVLKVLTG [1×Myr]
b <sub>9</sub>	531.4	2	GIGAVLKVL [1×Myr]
b <sub>10</sub>	582.1	2	GIGAVLKVLT [1×Myr]
b <sub>11</sub>	632.4	2	GIGAVLKVLT [1×Myr]
b <sub>12</sub>	661.1	2	GIGAVLKVLTG [1×Myr]
b <sub>11</sub> -H <sub>2</sub> O	623.6	2	GIGAVLKVLT [1×Myr]
b <sub>12</sub> -H <sub>2</sub> O	1302.8	1	GIGAVLKVLTG [1×Myr]
b <sub>12</sub> -H <sub>2</sub> O	652.5	2	GIGAVLKVLTG [1×Myr]

<sup>a</sup> Key: Myr, myristoyl; int, internal; <sup>b</sup> some observed *m/z* are very close matches to ions in both b and y sequence ladders and have been included in both

15

## Kinetics of the POPC Reaction

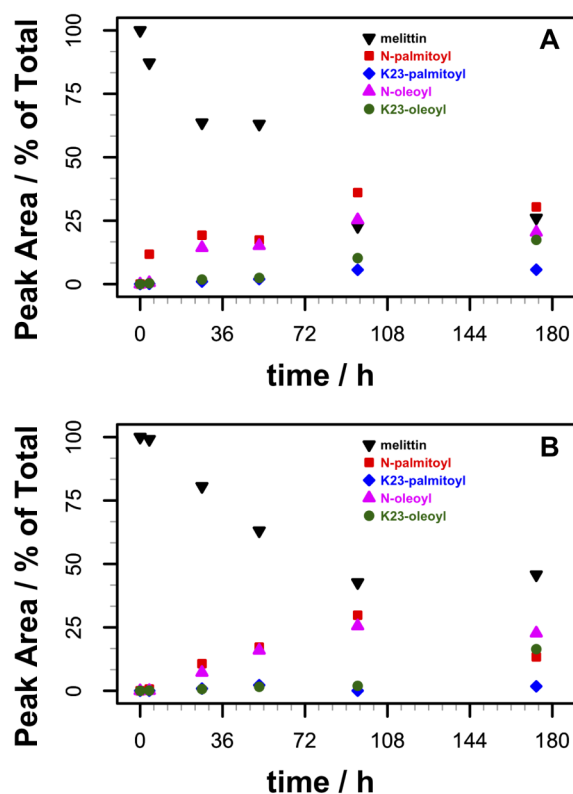
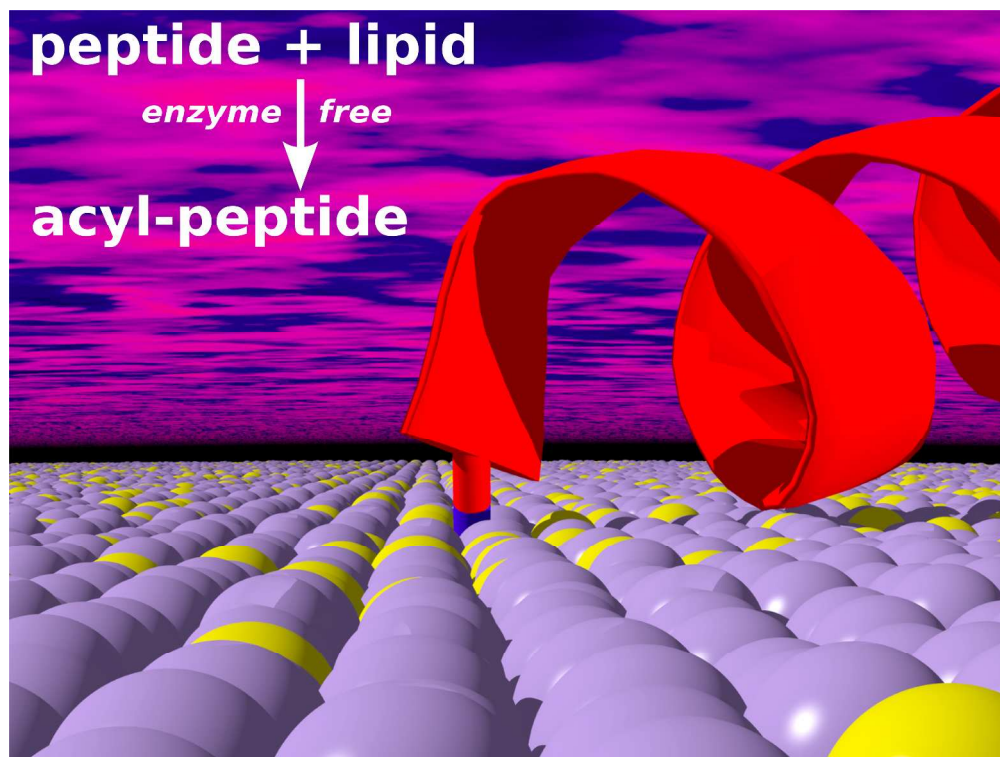


Fig. S14 Rates of formation and consumption of key species in the reaction of melittin with POPC (A) and OPPC (B). At each time point, the integrated area of each peak from the extracted ion chromatogram is determined as a percentage of the total integrated area for all peaks.

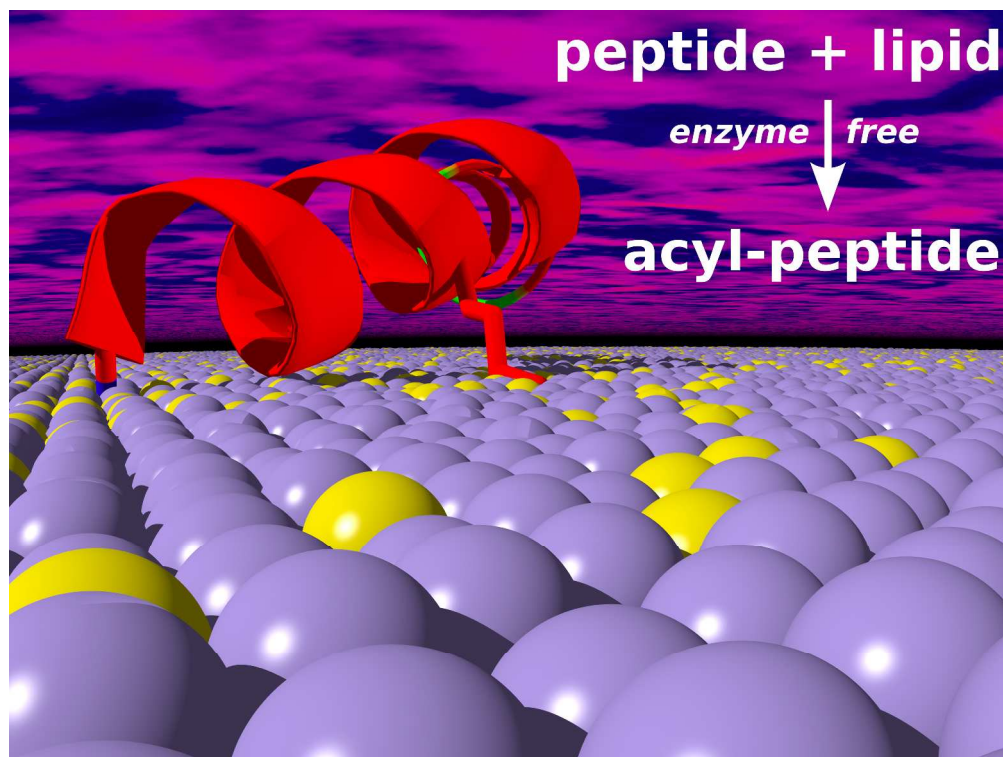
## Notes and references

<sup>10</sup> <sup>a</sup> Department of Chemistry, Biophysical Sciences Institute, Durham University, Durham, United Kingdom. Fax: +44 (0)1913844737; Tel: +44 (0)191 3730838; E-mail: j.m.sanderson@durham.ac.uk

- 1 Calculated using ProtParam ([www.expasy.ch/tools/protparam.html](http://www.expasy.ch/tools/protparam.html)) using a modified extinction coefficient for Trp according to Pace (C. N. Pace, F. Vajdos, L. Fee, G. Grimsley, and T. Gray, *Protein Sci.*, 1995, **11**, 2411).
- 2 H. P. Benton, D. M. Wong, S. A. Trauger, and G. Siuzdak, *Anal. Chem.*, 2008, **80**, 6382–6389.
- 3 R Development Core Team R: A language and environment for statistical computing, R Foundation for Statistical Computing, Vienna, Austria, 2008. (ISBN 3-900051-07-0, URL <http://www.R-project.org>).



Acyl transfer from lipids to a membrane-active peptide without enzyme catalysis



Acyl transfer from lipids to a membrane-active peptide without enzyme catalysis